Published online 26 June 2012 *Nucleic Acids Research, 2012, Vol. 40, No. 17* ***8499–8518***
doi:10.1093/nar/gks634

HnRNP A1 phosphorylated by VRK1 stimulates telomerase and its binding to telomeric DNA sequence

Yoon Ha Choi[1], Jong-Kwan Lim[1], Min-Woo Jeong[1] and Kyong-Tai Kim[1,2,*]

[1]Department of Life Science, Division of Molecular and Life Science, Pohang University of Science and Technology (POSTECH) and [2]Division of Integrative Bioscience and Biotechnology, Pohang University of Science and Technology (POSTECH), San-31, Hyoja-Dong, Pohang 790-784, Republic of Korea

Received September 8, 2011; Revised May 29, 2012; Accepted June 2, 2012

ABSTRACT

The telomere integrity is maintained via replication machinery, telomere associated proteins and telomerase. Many telomere associated proteins are regulated in a cell cycle-dependent manner. Heterogeneous nuclear ribonucleoprotein A1 (hnRNP A1), a single-stranded oligonucleotide binding protein, is thought to play a pivotal role in telomere maintenance. Here, we identified hnRNP A1 as a novel substrate for vaccinia-related kinase 1 (VRK1), a cell cycle regulating kinase. Phosphorylation by VRK1 potentiates the binding of hnRNP A1 to telomeric ssDNA and telomerase RNA *in vitro* and enhances its function for telomerase reaction. VRK1 deficiency induces a shortening of telomeres with an abnormal telomere arrangement and activation of DNA-damage signaling in mouse male germ cells. Together, our data suggest that VRK1 is required for telomere maintenance via phosphorylation of hnRNP A1, which regulates proteins associated with the telomere and telomerase RNA.

INTRODUCTION

The telomere is a unique structure that contains highly repetitive sequences; the terminus of mammalian telomeres consists of a 3′ single-stranded G-rich overhang (G-overhang), which represents the substrate for telomerase (1). The G-overhang is conserved throughout eukaryotic organisms from yeast to humans. Human telomeric DNA is composed of tandem repeats of 10–15 kb G-rich duplex sequences with G-rich 3′ overhang of approximately 130–210 nt (2–5). Telomere ends are protected from DNA damage signaling by t-loop structures formed via invasion of the single-stranded G-overhang into the double-stranded telomere repeats (6,7). Many proteins associate with telomeres to protect their length from DNA loss, end-to-end fusion and potential errors. In particular, the six-protein complex called shelterin (TRF1, TRF2, TIN2, Rap1, TPP1 and POT1) is endowed with specificity for telomeric sequences (5,7,8).

The generation of the G-overhang is dynamically regulated with the cell cycle (9,10). In telomerase positive cells, the length of the G-overhang transiently increases in late S/G2 phase (11). A recent study showed that global G-overhang length gradually increased during S phase in both telomerase-positive and -negative cells, demonstrating that the production of the G-overhang is telomerase-independent (12). Dai *et al.* suggested that overhangs at the leading telomere are gradually lengthened during S∼G2/M phase via DNA extension and 3′ strand resection (12,13). On the other hand, overhangs at the lagging telomere are lengthened in S phase and then shortened at late S/G2 phase, caused by delayed C-strand fill-in. This late S/G2-specific C-strand fill-in requires lagging strand synthesis machinery, which may be regulated by CDK1 (12,14,15).

Telomere has crucial function for the preservation from the activation of the DNA damage response by the exposure of chromosome end (5). The telomeric G-overhang is covered with RPA in S phase, contributing to DNA replication and recruitment of ATR (16). RPA is displaced with POT1, which suppresses ATR activation and the DNA damage response (17). As POT1 cannot out-compete RPA binding on G-overhangs, it has been suggested that other proteins control the RPA-to-POT1 switch (18). A recent study identified heterogeneous nuclear ribonucleoprotein (hnRNP) A1 as the RPA displacement factor, which actively plays a role at post S phase (18).

*To whom correspondence should be addressed. Tel: +82 54 279 2297; Fax: +82 54 279 2199; Email: ktk@postech.ac.kr

HnRNPs have been identified as binding proteins for telomerase RNA and telomeric ssDNA oligonucleotides (19–23). The hnRNP A1, A2-B1, D and E and hnRNP homologous proteins can interact with the single-stranded telomeric repeat sequence *in vivo* (24,25). Of these factors, hnRNP A1 is known to play a critical role in telomere biogenesis. Although hnRNP A1 is abundant in the eukaryotic nucleus and its role in mRNA processing is well understood, important evidence for its function in telomere regulation has been also reported. First, hnRNP A1 is critical for the maintenance of telomere length. Chabot and colleagues showed that an hnRNP A1-deficient murine erythroleukemia cell line restored telomere length by the addition of hnRNP A1 or its shortened derivative, UP1 (23). Second, hnRNP A1/UP1 binds to telomerase RNA and appears to stimulate telomerase activity via unwinding of the G-quadruplex structures of telomere (26,27).

Several studies have reported that hnRNP A1 is regulated by post-translational modification (28–33), however its physiological function in telomere structure has not been well understood. Here, we provide evidence that phosphorylation of hnRNP A1 enhances its binding to telomeric ssDNA and potentiates its function for telomerase reaction. We demonstrate, for the first time, that vaccinia-related kinase 1 (VRK1), which participates in cell cycle progression, phosphorylates hnRNP A1 *in vitro* and *in vivo* and regulates G-overhang length. Also, testicular germ cells in a VRK1-deficient mouse showed an abnormality in telomere integrity. Taken together, our data provide further evidence that VRK1 participates in telomere maintenance by regulating the function of hnRNP A1.

MATERIALS AND METHODS

Plasmids and proteins

HnRNP A1 protein was obtained using the IMPACT^{TM}-CN system (New England Biolabs). HnRNP A1 cDNA was inserted to the pTYB2 vector for purifying hnRNP A1 protein. pTYB2–hnRNP A1 was transformed in *Escherichia coli* BL21 following protein induction by adding 0.3 mM of IPTG. Non-tagged hnRNP A1 protein was eluted under reducing conditions (0.5 mM DTT/pH 8.0). To rescue of VRK1 for the knock-down of VRK1, siRNA resistant gene which contains silent mutation was generated. To fully abolish the siRNA effect, two nucleic acids in each siRNA-targeted regions were mutated.

In vitro and *in vivo* kinase assays

The *in vitro* kinase assay was performed with 0.5 μg of recombinant GST-VRK1 protein and 0.25, 0.5 or 0.8 μg of hnRNP A1 protein containing 20 mM Tris–HCl, pH 7.5, 5 mM $MgCl_2$, 150 mM KCl and 5 mCi of γ^{32}P-ATP. The reaction was performed for 30 min at 37°C.

To knock down VRK1, HeLa cells were transfected with negative control siRNA or siRNA against hVRK1 (siGENOME SMARTpool M-004683; Dharmacon) by electroporation (NEON® transfection system; Invitrogen) and incubated in DMEM with 10% fetal bovine serum for 16 h. For the *in vivo* kinase assay, cells were incubated in phosphate-free DMEM (Invitrogen) containing 10% dialyzed fetal bovine serum and 0.25 mCi [^{32}P] phosphate/ml for 24 h. Cells were harvested and equal amounts of lysate were used for immunoprecipitation of hnRNP A1. Samples were separated using sodium dodecyl sulfate polyacrylamide gel electrophoresis (SDS–PAGE), following transfer to nitrocellulose membrane. Phosphorylated hnRNP A1 was detected using autoradiography and the hnRNP A1-specific band was confirmed with Western blotting using anti-hnRNP A1 antibody (SC-32301; Santa Cruz Biotechnology).

Direct telomerase activity assay and real-time quantitative telomeric repeat amplification protocol assay

For the preparation of hnRNP A1-depleted telomerase extract, hnRNP A1 proteins were affinity-depleted by incubation of telomerase extract from A549 cell line with 3′-biotinylated Telo7 [$(TTAGGG)_7$] oligonucleotide as earlier described (26). Partial enrichment of telomerase complex, nuclear extract of A549 cell (1×10^9 cells/ml) was fractionated using 10–40% glycerol gradient and concentrate protein to 10-fold using Vivaspin® 500 column (Sautorious). Telomerase activity was confirmed using TRAP assay in each fraction, telomerase enriched fraction was used for direct telomerase activity assay. The 50 μl reaction mixture contained 20 mM Tris–Cl (pH 8.3), 1.5 mM $MgCl_2$, 63 mM KCl, 0.05% (v/v) Tween 20, 1 mM EGTA, 1 mM dATP, 1 mM dTTP, 10 μM dGTP, 100 μCi [α-^{32}P]-dGTP, 100 pmol 5′-biotin-CTAGACCTGTCATCA$(TTAGGG)_3$-3′, 10 μl hnRNP A1-depleted telomerase extract. hnRNP A1 or hnRNP A1 S6A mutant proteins were added as a indicated concentration. Samples were incubated 1 h at 37°C for the synthesis of telomerase product and phosphorylation of hnRNP A1. Biotinylated telomerase product was precipitated using streptavidin bead and analyzed by electrophoresis on a 10% polyacrylamide/7 M urea gel. To confirm the phosphorylation of hnRNP A1 in a assay condition, 0.5 μg of hnRNP A1 was incubated in a assay condition with 5 mCi of γ^{32}P-ATP. HnRNP A1 was precipitated with 1 μg of anti-hnRNP A1 antibody conjugated with protein G bead. The immune-complexes were fractionated on SDS–PAGE, and exposed to X-ray film. Gel was stained by SYPRO® Ruby protein gel staining solution (Invitrogen).

Quantitative telomeric repeat amplification protocol (Q-TRAP) with real time polymerase chain reaction is well described by Herbert *et al.* (34). Lysates from testis or the cell line were obtained by lysis with NP-40 buffer. For the standard curve, the A549 cell lysate was used. Testicular lysates from wild-type and VRK1-deficient mice were incubated with Q-TRAP reaction mix for 30 min at room temperature (RT) for extension of the substrate by telomerase. Quantitative polymerase chain reaction was performed using the StepOne Plus^{TM} system (Applied Biosystems). Sample data was converted into relative telomerase activity (RTA) units that are

defined by the standard curve and the linear equation [RTA of sample = $10(C_t$ sample $- Y_{int})$/slope].

Immunohistochemistry

WT and VRK1 testes were fixed in 4% paraformaldehyde, dehydrated using an ethanol series and embedded in paraffin. Sectioned tissues (5 μm) were dehydrated and stained with anti-mouse VRK1 antibody and anti-hnRNP A1 antibody. After staining with specific antibody, the samples were treated with anti-mouse alexa 594 and anti-rabbit alexa 488 antibodies.

Electrophoretic mobility shift assay

For the kinase reaction, hnRNP A1 was incubated with GST-hVRK1 in kinase buffer (50 mM Tris–Cl, pH 7.5, 10 mM $MgCl_2$, 1 mM DTT and 50 mM KCl) for 30 min at 37°C. All other samples were mixed with the same kinase buffer. After brief cooling on ice, samples were added to electrophoretic mobility shift assay reaction buffer (4% glycerol, 0.5 mM EDTA, 50 mM NaCl and 0.05 mg/ml poly dI-dC) and ^{32}P-labeled Telo7 oligonucleotide [$(TTAGGG)_7$], and then incubated at 4°C for 20 min. The complex of hnRNP A1 and probe was confirmed by adding anti-hnRNP A1 antibody (SC-32301; Santa Cruz Biotechnology). Samples were loaded onto a 5% native acrylamide gel and separated at 200 V at 4°C.

DNA-protein binding assay using biotinylated ssDNA

Biotinylated ssTEL [Telo7; $(TTAGGG)_7$] or TERRA [$(UUAGGG)_3$] was attached to streptavidin-coated beads (Thermo, #20349) in binding buffer at RT for 20 min. For the kinase reaction of VRK1 and hnRNP A1, 1 μg of hnRNP A1 was incubated with 1 μg of GST-hVRK1 at 37°C with ATP and kinase buffer. For the non-kinase reacted control, hnRNP A1 was incubated at 37°C without GST-VRK1 in a same condition. Indicated amount of HnRNP A1 or kinase-reacted hnRNP A1 proteins were incubated with biotinylated ssTEL-streptavidin bead in binding buffer (10 mM Tris–HCl (pH 7.5), 100 mM NaCl, 10% glycerol, 0.05% NP-40) for 20 min at room temperature. After several washing, bound hnRNP A1 was separated using SDS–PAGE and detected by Western blot. To quantify the hnRNP A1 band obtained by Western blot analysis, we applied ImageJ software-based analysis (http://rsb.info.nih.gov/ij/).

TRF assay

For the terminal restriction fragment (TRF) assay, mouse testicular genomic DNA (gDNA) was prepared by phenol–chloroform extraction. Three micrograms of gDNA were cleaved with 10 U RsaI and 10 U of HinfI at 37°C. Samples were separated in a 0.5% agarose gel with 1 × TAE buffer and were run overnight (~20 h) at 2 V cm^{-1}. The gel was then exposed to denaturation solution (0.5 M NaOH/1.5 M NaCl) for 30 min followed by neutralization solution (1.5 M NaCl/0.5 M Tris) for 30 min. DNA was transferred to Biodyne B (Pall) membrane and cross-linked in UV-cross linker. The membranes were hybridized with ^{32}P-labeled anti-Tel3 probe [$(CCCTAA)_3$] at 42°C and washed several times. Autoradiographs were detected with X-ray film.

Immunoprecipitation

For the immunoprecipitation of telomerase complex, A549 cell lysate was incubated with 1 μg of anti-telomerase protein (TERT) antibody (Santa Cruz biotechnology, sc-7212). To detect telomerase RNA in telomerase complex, elution buffer (100 mM Tris–Cl, pH 8, 10 mM Na_2-EDTA and 1% SDS in DEPC water) was added to precipitate following incubation for 10 min at 37°C. For the reverse crosslink, 0.2 M NaCl and 3 mg/ml Proteinase K were added to eluent and incubated for 30 min at 55°C. After the phenol–chloroform extraction, RNA was precipitated using ethanol. Telomerase RNA was detected by RT-PCR using a gene-specific primer (the length of RT-PCR product is 184 bp, forward: 5′-CCTGCCGCCT TCCACCGTTC-3′, reverse: 5′-CTGACAGAGCCCAAC TCTTCGC-3′). For the quantify control, GAPDH gene was detected (forward: 5′-ACCACAGTCCATGCCATC AC-3′, reverse: 5′-TCCACCACCCTGTTGCTGTA-3′).

Telomere-fluorescence *in situ* hybridization analysis

Cross-sections of mouse testes were de-paraffinized then treated with 20 μg/ml proteinase K for 10 min at RT. After washing in phosphate buffered saline (PBS), sections were dehydrated with a 70–100% ethanol series. Sections were stained with fluorescein isothiocyanate-labeled telomeric DNA probe of $[TTAGGG]_3$ (PANAGENE) in hybridization buffer (10 mM $NaHPO_4$, pH 7.4, 10 mM NaCl, 20 mM Tris, pH 7.5 and 70% formamide), followed by denaturation at 80°C for 5 min and hybridization for 30 min at RT. Samples were washed with wash buffer I (PBS/0.2% Tween-20) and wash buffer II (2 × SSC/0.1% Tween-20) and then counterstained with Hoechst 33342 in PBS for 10 min.

3′ overhang analysis

Telomeric-oligonucleotide ligation assay (T-OLA) was performed as previously described (35). Briefly, 5 μg gDNA was hybridized with ^{32}P-labeled $(CCCTAA)_3$ for 12 h at 50°C, followed by ligation with 40 U Taq ligase for 5 h at 50°C. Samples were extracted with phenol–chloroform and then precipitated. The dried DNA pellet was resuspended in a formamide based loading buffer and electrophoresed onto an 8% acrylamide/6 M urea gel. The gel was dried and radioactivity was detected by exposing to X-ray film.

3′ overhang was also measured by TRF analysis in native gel conditions. Genomic DNA in S phase and G2 phase cells were reacted with restriction enzymes (HinfI, HaeIII and MspI) and separated in 0.7% agarose gel by electrophoresis. gDNA was transferred to positive charged nylon membrane by traditional capillary transfer method. Membrane was hybridized with ^{32}P-labeled $(CCCTAA)_3$ and exposed to X-ray film. For detect the total telomere, membrane was denaturated in 0.4 N NaOH for 5 min and briefly washed with 2 × SSC. Membrane was hybridized with ^{32}P-labeled $(CCCTAA)_3$ and exposed to X-ray film.

Telomere-ChIP

Testicular cells from wild-type and VRK1-deficient mice were prepared (2×10^7 cells) for each reactions and sonicated six times (Amplitude 60, Output 7, 30 s of Sonic following 1 min of rest) to generate DNA fragments. Immunoprecipitation was carried out 16 h at using antibodies against hnRNP A1 (mAb 4B10; Santa Cruz biotechnology, K350; Cell Signalling Technology; R196; Cell Signalling Technology). For negative control, IgG was incubated with cell lysate. Precipitated DNA was blotted on Biodyne B (Pall) membrane using Bio-Dot® Microfiltration apparatus (BIO-RAD). Probes used were ^{32}P-labelled oligonucleotides specific for telomeric repeats $(TTAGGG)_7$ and major satellite repeats (5′-TAT GGC GAG GAA AAC TGA AAA AGG TGG AAA ATT TAG AAA TGT CCA CTG TAG GAC GTG GAA TAT GGC AAG-3′), respectively.

RESULTS

HnRNP A1 as a novel substrate for VRK1

In studies of the interacting proteins of VRK1, we observed that hnRNP A/B bound to VRK1 (data not shown). We verified the interaction between hnRNP A1 and VRK1 by immunoprecipitation and GST-pull down assay. In Figure 1A, over-expressed hVRK1 co-precipitated with hnRNP A1. To determine whether hnRNP A1 and VRK1 interact directly, a GST-pull down assay was performed. Figure 1B shows that recombinant GST-hVRK1 and hnRNP A1 proteins interact directly (Figure 1B). Next, we determined whether hnRNP A1 is a substrate for VRK1 using an *in vitro* kinase assay. In Figure 1C, recombinant hnRNP A1 protein was strongly phosphorylated by GST-hVRK1.

Enhanced binding of phosphorylated hnRNP A1 to telomeric ssDNA

To investigate whether phosphorylation of hnRNP A1 by VRK1 affected binding to telomeric DNA sequences, we performed gel retardation assays. First, we validated the specific interaction between the recombinant hnRNP A1 protein and telomeric DNA probe by a supershift gel assay using anti-hnRNP A1 antibody or non-specific antibody (Supplementary Figure S1). In Figure 2A, hnRNP A1 was reacted with VRK1 in the presence or absence of ATP, followed by incubation with ^{32}P-labeled telomeric ssDNA. In the reaction condition with ATP, the signal intensity of the complex was stronger than the reaction condition without ATP (Figure 2A). The complex of hnRNP A1 and telomeric ssDNA probe was confirmed with anti-hnRNP A1 antibody (Figure 2A, lane 3 and 7). To quantify the binding affinity, cold telomeric ssDNA probe was added to hnRNP A1 and ^{32}P-telomeric probe for the competition assay (Figure 2B). When we added none or low concentrations of cold telomeric ssDNA, several highly retarded complexes appeared, and smaller complexes appeared as the cold telomeric ssDNA increased. This is consistent with the binding assays of UP1 (an N-terminal proteolytic fragment of hnRNP A1) and telomeric ssDNA, which showed multiple retarded bands when the concentration of UP1 protein was increased (24,26,36). In Figure 2B, the affinity was determined by calculating the concentration of cold oligonucleotide required to block 50% of hnRNP A1 to ^{32}P-telomeric ssDNA and presented as $Telo_{50}$. As a result, the binding affinity of hnRNP A1 ($Telo_{50}$ = 15 pmol) which was reacted with VRK1 was higher than non-reacted hnRNP A1 ($Telo_{50}$ = 3.28 pmol).

To verify the enhanced binding of VRK1-phosphorylated hnRNP A1, we also tested its binding using an *in vitro* biotinylated ssDNA-protein binding assay. Biotinylated telomeric ssDNA oligonucleotide was incubated with hnRNP A1, which was phosphorylated by VRK1 or not. As seen in Figure 2C, phosphorylated hnRNP A1 more intensively bound to the oligonucleotide in an hnRNP A1-concentration-dependent manner (Figure 2C). These data show that phosphorylation by VRK1 potentiated the binding of hnRNP A1 to telomeric DNA sequences *in vitro*.

Binding of hnRNP A1 to telomeres can be regulated by telomeric repeat-containing RNA (TERRA) (18). We examined whether phosphorylation of hnRNP A1 affected binding to the TERRA and found that hnRNP A1 binding to the TERRA was not significantly changed after phosphorylation by VRK1, but seemed to be slightly reduced (Figure 2D). Next, we checked the rate of hnRNP A1 sequestration from the telomeric oligonucleotide by TERRA. TERRA was incubated with either hnRNP A1-coated telomeric oligonucleotide or kinase-reacted hnRNP A1-coated telomeric oligonucleotide (Telo7). After several washings, the amount of hnRNP A1 remaining on telomeric oligonucleotide was detected by Western blotting. In Figure 2E, more hnRNP A1 remained bound to Telo7 following the kinase reaction with VRK1. This result shows that VRK1-phosphorylated hnRNP A1 is less competed by TERRA than the non-phosphorylated form.

VRK1-mediated phosphorylation of hnRNP A1 *in vivo* and identification of the phosphorylation site

Since hnRNP A1 is target protein that is regulated by several kinases, we wanted to confirm whether hnRNP A1 is phosphorylated by VRK1 *in vivo*. To measure the phosphorylation of hnRNP A1, A549 cells which were transfected with negative control siRNA (siCont) or siRNA against VRK1 (siVRK) and were incubated with ^{32}P-inorganic phosphate. HnRNP A1 was precipitated with anti-hnRNP A1 antibody and then the phosphorylation signal was detected by autoradiogram. In Figure 3A, phosphorylation of hnRNP A1 was significantly reduced after VRK1 depletion (Figure 3A). This result suggests that VRK1 phosphorylates hnRNP A1 *in vivo*.

It has been reported that hnRNP A1 is phosphorylated at Ser 95 and Ser 192 by DNA-PK and Ser 192 and Ser 310–312 by mitogen-activated protein kinase signal-integrating kinase (Mnk) (33,37). To estimate the phosphorylation site on hnRNP A1 by VRK1, we used the prediction program of kinase-specific phosphorylation site (GPS2.0: http://gps.biocuckoo.org/)

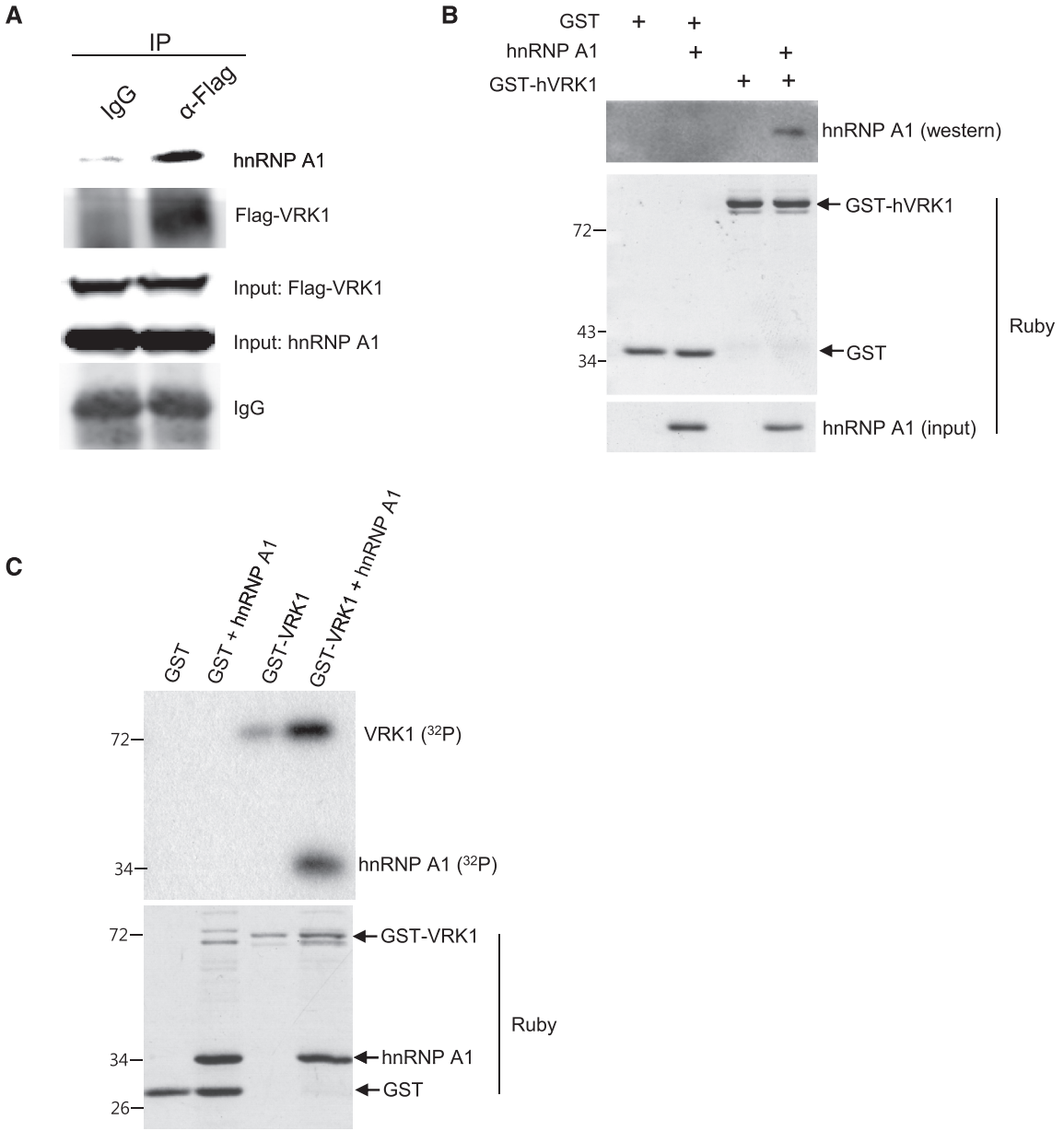

Figure 1. Phosphorylation of hnRNP A1 by VRK1. (**A**) HnRNP A1 interacts with VRK1. Flag-VRK1 was over-expressed in HeLa cells and immunoprecipitated with anti-Flag antibody. Cell extracts were prepared as described in the 'Materials and Methods' section. (**B**) Recombinant GST-hVRK1 and hnRNP A1 proteins were incubated and pulled-down with glutathione sepharose beads. Binding of GST-hVRK1 and hnRNP A1 was confirmed with immunoblotting of hnRNP A1. Input proteins (GST-hVRK1, GST and hnRNP A1) are confirmed by SYPRO® Ruby staining. (**C**) VRK1 phosphorylates hnRNP A1. GST, GST-VRK1 and hnRNP A1 input proteins are stained by SYPRO® Ruby stain.

(38). This program classifies protein kinases with their verified sites into a hierarchical structure with four levels, including group, family, subfamily and single protein kinase (39). Examination of the amino acid sequence of hnRNP A1 revealed two candidate sites, Ser 6 and Ser 158. To confirm whether these sites are phosphorylated by VRK1, we generated hnRNP A1 mutants with substitution of Ala for Ser at Ser 6 or Ser 158. Mutant hnRNP A1 proteins were reacted with VRK1 *in vitro* and as a result, phosphorylation of hnRNP A1 was significantly reduced in the S6A mutant (Figure 3B). Because the phosphorylation signal in the S6A mutant did not completely disappear, we speculated that VRK1 also simultaneously phosphorylates another site. To assess whether phosphorylation at Ser 6 is significant for binding of hnRNP A1 to telomeric ssDNA, hnRNP A1 S6A mutant and wild-type hnRNP A1 proteins were incubated with 3′-biotinylated Telo7. The results showed that the S6A mutant hnRNP A1 did not demonstrate increased binding to telomere ssDNA after the kinase reaction with VRK1 (Figure 3C). Together, these results indicate that VRK1 phosphorylates hnRNP A1 at Ser 6, which is critical for the enhancement of binding to telomeric ssDNA.

Enhanced binding of phosphorylated hnRNP A1 to telomerase RNA

It has been reported that hnRNP A1 also binds to the human telomerase RNA (hTR) and controls the activity of telomerase (26,27). We asked whether VRK1 also affected the binding of hnRNP A1 to telomerase RNA. hnRNP A1 and phosphorylated hnRNP A1 proteins were incubated with hTR 15mer (residues 56–71 of telomerase RNA) and analyzed by gel retardation assay. In Figure 4A, hnRNP A1 bound to the hTR 15mer and phosphorylation of hnRNP A1 enhanced the binding to the hTR. Phosphorylation of hnRNP A1 was confirmed by duplicated kinase reaction using ^{32}P-ATP (Supplementary Figure S2A). The affinity was determined by calculating the concentration of cold oligonucleotide required to block 50% of hnRNP A1 to ^{32}P-hTR and presented as hTR_{50} (Figure 4B). As a result, the binding affinity of hnRNP A1 (hTR_{50} = 2.46 pmol) which was reacted with VRK1 was higher than non-reacted hnRNP A1 (hTR_{50} = 0.51 pmol). We also confirmed that VRK1 affected the interaction of hnRNP A1 and telomerase

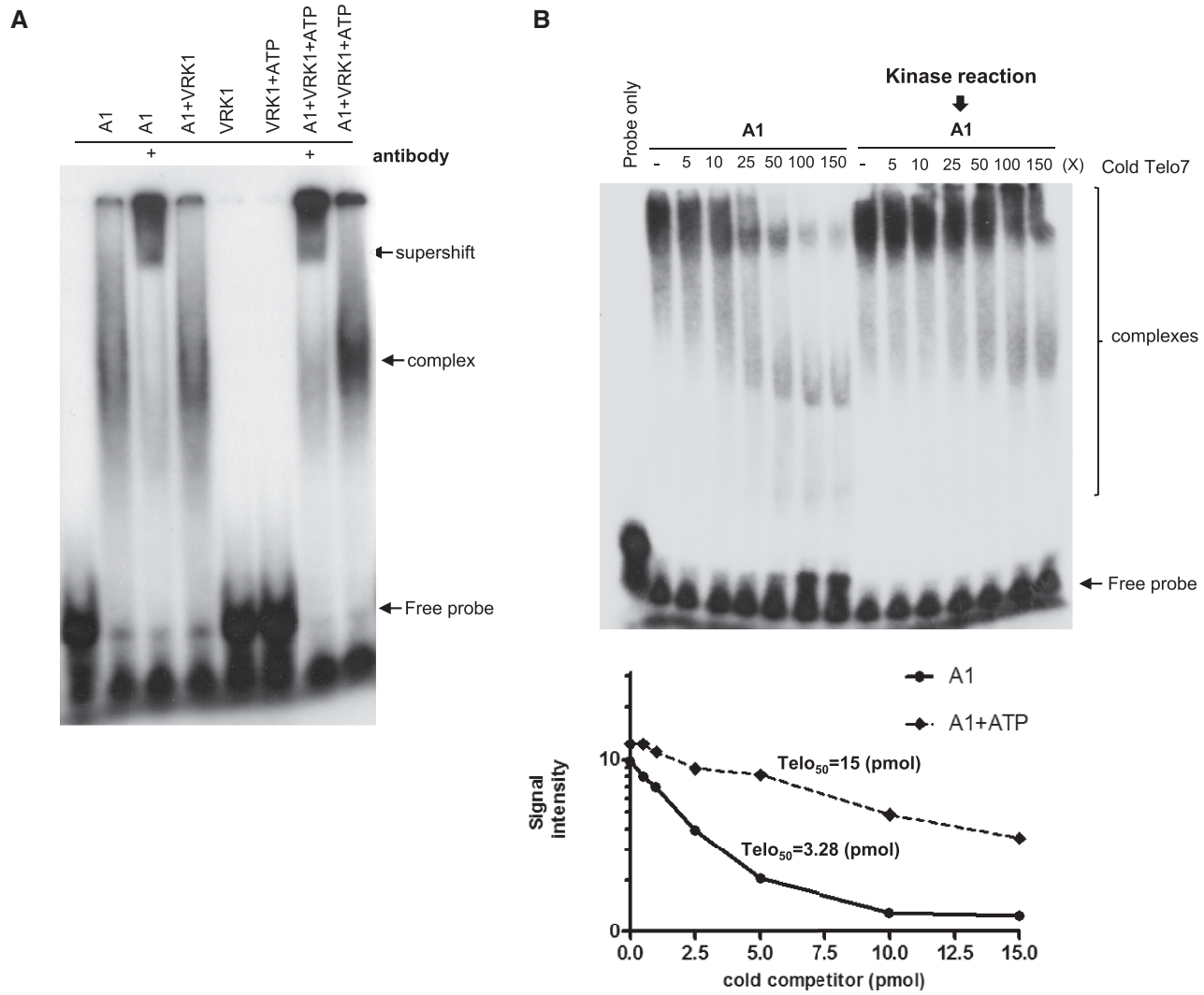

Figure 2. VRK1 enhances the binding of hnRNP A1 to telomeric DNA. (**A**) Phosphorylation of hnRNP A1 by VRK1 enhances binding to the telomeric oligonucleotide. HnRNP A1 or VRK1 phosphorylated hnRNP A1 was incubated with ^{32}P-Telo7 probe. hnRNP A1 protein was incubated with VRK1 without (lane 4) or with ATP (lane 7 and 8) for phosphorylation prior to oligonucleotide-binding. The complex of hnRNP A1 and Telo7 was confirmed by supershift (lane 4 and 7). (**B**) The binding affinity of HnRNP A1 protein or kinase-reacted hnRNP A1 protein with telomeric ssDNA was confirmed by competitive EMSA assay. A total of 0.1 pmol of 32 P-Telo7 probe was bound with hnRNP A1 or kinase-reacted hnRNP A1 protein in each conditions and cold-Telo7 oligonucleotide was added as indicated in **B**. The signal intensity was plotted and the binding affinity was calculated in lower panel. (**C**, **D**) HnRNP A1 or kinase-reacted hnRNP A1 was incubated with biotinylated Telo7 (**C**) or TERRA (**D**), followed by precipitation with streptavidin beads. Binding of hnRNP A1 protein to the telomeric oligonucleotide was confirmed by immunoblotting with anti-hnRNP A1 antibody. Phosphorylation of hnRNP A1 is detected by autoradiography (^{32}P). The results from individual experiments (n = 3) were plotted (bottom panel). Error bars represent standard deviation. (**E**) HnRNP A1 or hnRNP A1 reacted with VRK1-coated Telo7 was incubated with increasing concentrations of TERRA (25, 50 and 100 pmol). The remaining hnRNP A1 on Telo7 was detected by western blotting. Phosphorylation of hnRNP A1 is detected by autoradiography (^{32}P). The results from individual experiments (n = 3) were plotted (bottom panel). Error bars represent standard deviation.

(continued)

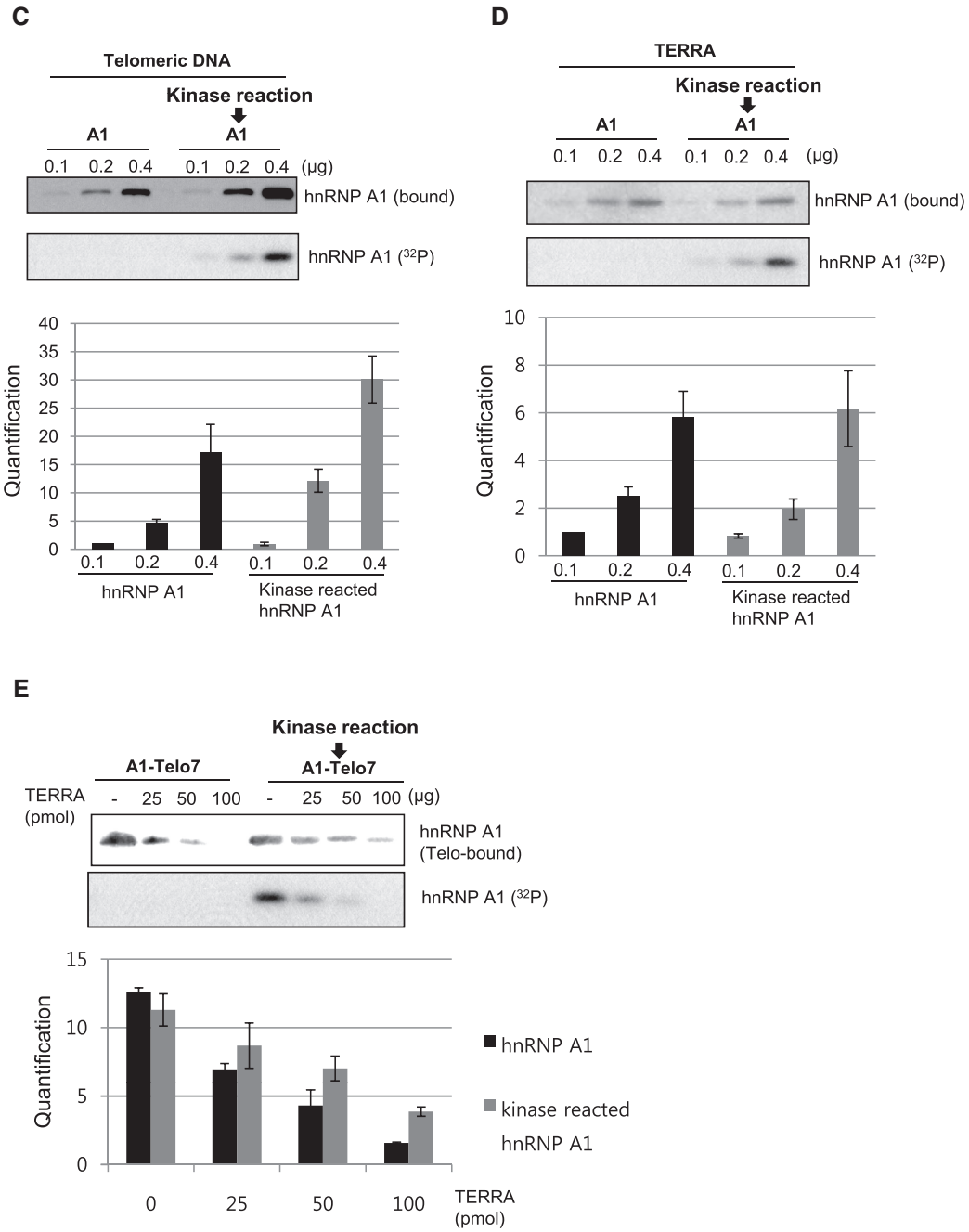

Figure 2. Continued.

in vivo using a co-immunoprecipitation assay (Figure 4C). Telomerase complex was precipitated using TERT antibody and confirmed by the detection of telomerase RNA in the precipitate (Supplementary Figure S2C). To reduce the expression of VRK1, A549 cells were transfected with siRNA against VRK1. Telomerase was immunoprecipitated with anti-TERT antibody, followed by immunoblotting of hnRNP A1. In Figure 4C, reduction of VRK1 resulted in a significant decrease in the interaction between hnRNP A1 and telomerase. To exclude the off-target effect of siRNA against VRK1, we generated Flag-CMV2-VRK1 construct containing silent mutations on the siRNA targeting sequences (Supplementary Figure S2B). For the add-back of VRK1, A549 cells were transfected with siVRK1 and Flag-CMV2-VRK1, simultaneously. Expression of Flag-CMV2-VRK1 was confirmed with anti-VRK1 antibody and anti-Flag antibody. In Figure 4C lane 2, reduced binding of hnRNP A1 onto the telomerase complex by siVRK1 was recovered when Flag-CMV2-VRK1 was ectopically expressed. Therefore, these results suggest that VRK1 affects the binding of hnRNP A1 to the telomerase complex *in vivo*.

To assess whether phosphorylation at Ser6 is significant for the activation of telomerase, hnRNP A1 or hnRNP A1

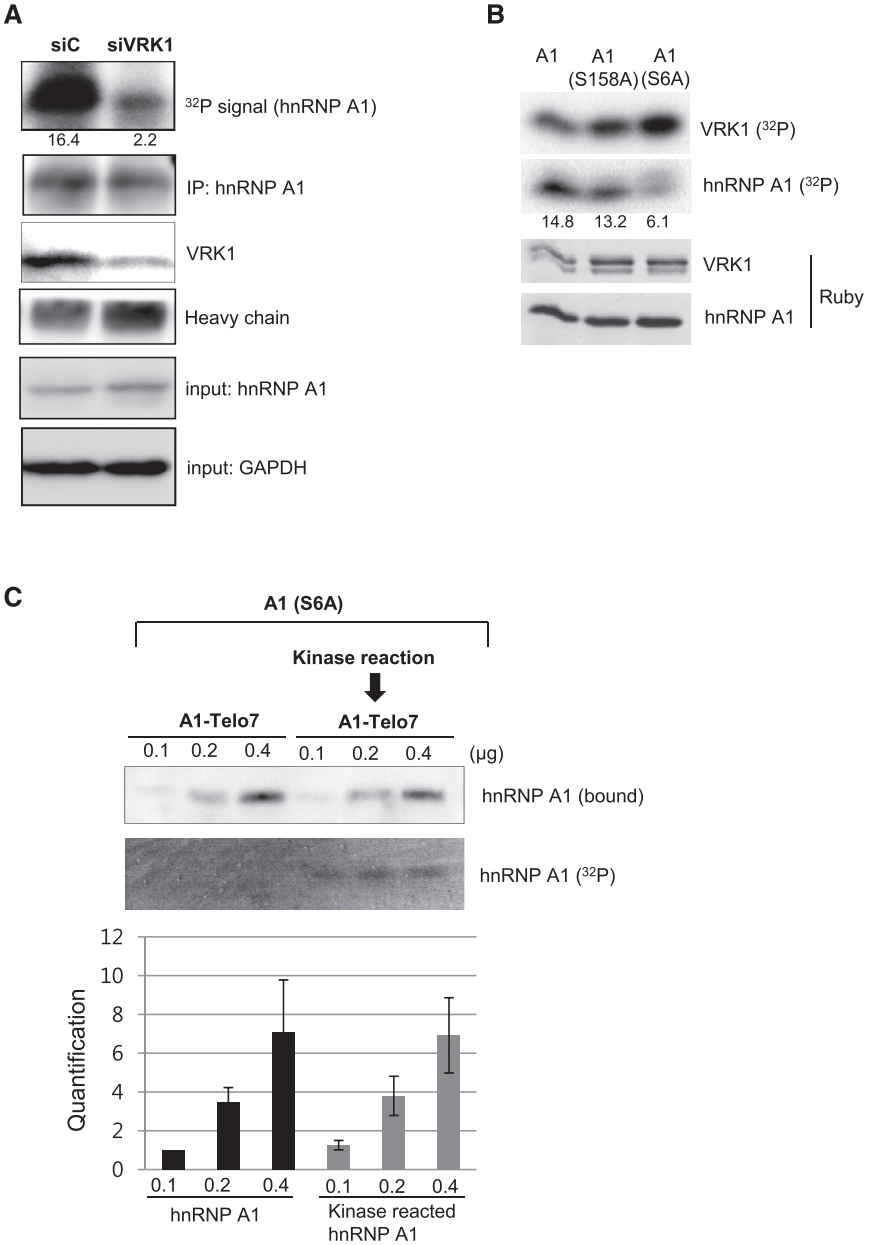

Figure 3. Identification of the VRK1-mediated phosphorylation site of hnRNP A1. (**A**) A549 cells were treated with negative control siRNA (siC) or VRK1 siRNA (siVRK1), then incubated with inorganic ^{32}P-phosphate. Cell lysates were incubated with anti-hnRNP A1 antibody for immunoprecipitation and ^{32}P signal on hnRNP A1 protein was analyzed after exposing to X-ray film. Total precipitated hnRNP A1 was detected by western blotting. (**B**) hnRNP A1 or hnRNP A1 mutants (S158A and S6A) was incubated with VRK1 under kinase reaction condition and ^{32}P-incorporation into hnRNP A1 and VRK1 was detected by autoradiography. The levels of hnRNP A1 and VRK1 were identified with SYPRO® Ruby staining. (**C**) HnRNP A1 S6A (0.1, 0.2 and 0.4 ng) or VRK1 phosphorylated hnRNP A1 S6A (0.1, 0.2 and 0.4 ng) were incubated with 10 pmol 3′-biotinylated Telo7. HnRNP A1 protein remaining on Telo7 was detected with western blotting. Phosphorylation of hnRNP A1 is detected by autoradiography (^{32}P). The results from individual experiments (n = 3) were plotted (bottom panel). Error bars represent standard deviation.

S6A mutant proteins were added back to hnRNP A1-depleted cell lysate. We confirmed the depletion of hnRNP A1 from a lysate by western blotting (Figure 4D). Consistent with previous observation, telomerase activity was significantly reduced in the hnRNP A1-depleted lysate (Figure 4D, 'bottom' panel) (26). Samples were incubated at 37°C allowing synthesis of telomerase product and phosphorylation of hnRNP A1, followed by the precipitation of biotinylated telomerase product. Phosphorylation of hnRNP A1 in this experimental condition was confirmed by autoradiography of hnRNP A1 (Supplementary Figure S3A). The amount of telomerase in each reaction was detected by TERT antibody (Supplementary Figure 3B). Consistent with previous report (26), hnRNP A1 promoted telomerase reaction in a concentration-dependent manner (Figure 4E). However, hnRNP A1 S6A mutant did not significantly stimulate telomerase action compared to WT

hnRNP A1 protein (Figure 4E). This result shows that phosphorylation of hnRNP A1 at Ser6 is important for stimulation of the telomerase reaction.

VRK1 affects G-overhang length during the cell cycle

A previous study had shown that total G-overhang length is transiently increased during late S/G2 phase in telomerase-positive cells (11). To determine whether VRK1 affected telomere G-overhang dynamics, we transfected A549 cells with negative control siRNA or siVRK1 (Supplementary Figure S3C) and synchronized cells using a double-thymidine block at the boundary period of G1/S phase (Figure 5). Cells were released from the block and collected at the indicated times. To measure G-overhang length, genomic DNA from the cells was subjected to the T-OLA. Consistent with the previous finding, the length of G-overhang gradually increased up to G2 phase (6 and

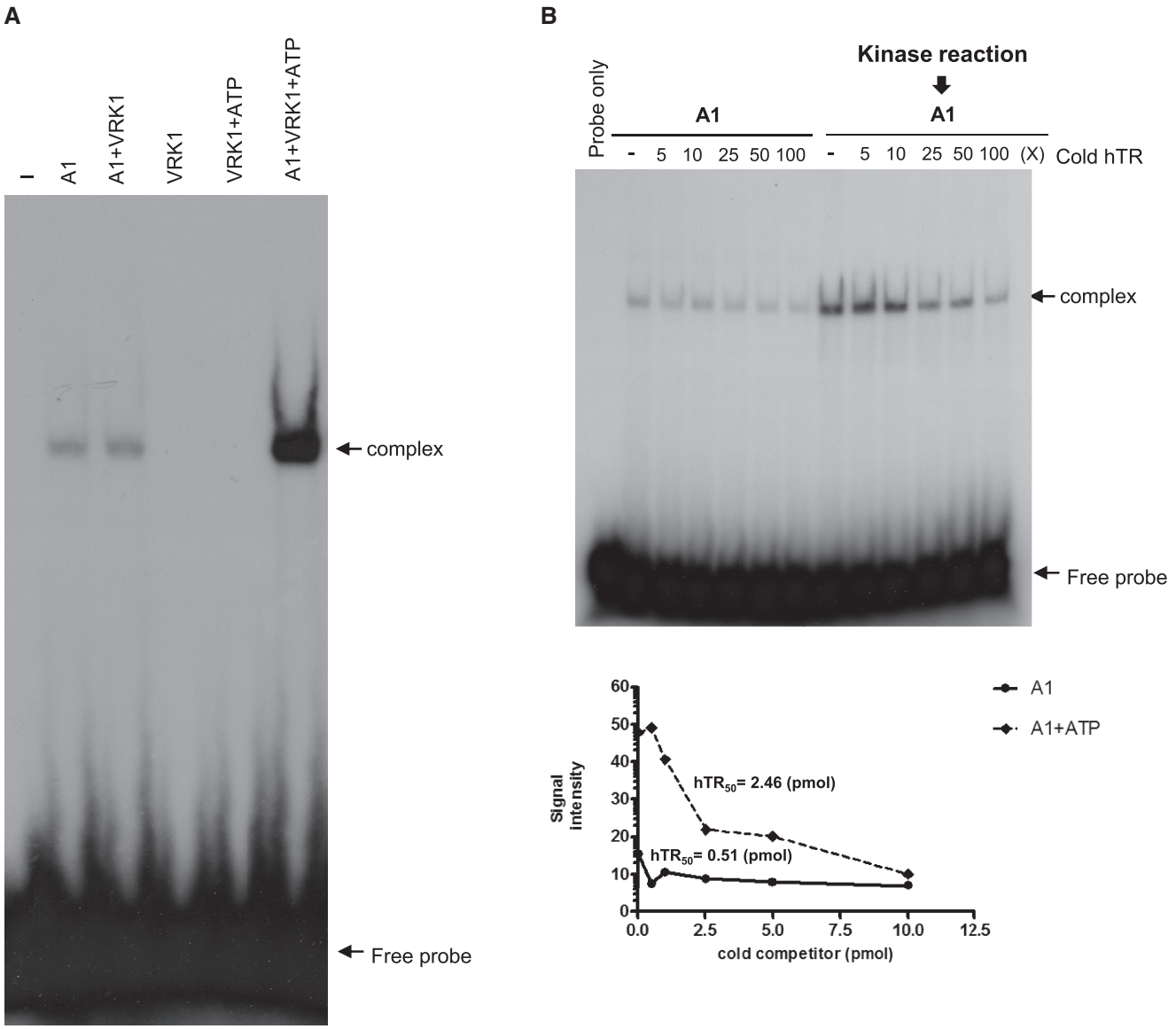

Figure 4. VRK1 enhances the binding of hnRNP A1 to hTR. (**A**) Phosphorylation of hnRNP A1 via VRK1 potentiated binding to hTR. A total of 0.5 and 1 μg hnRNP A1 protein or kinase-reacted hnRNP A1 (−ATP or +ATP) was incubated with the labeled hTR 15mer. (**B**) The binding affinity of hnRNP A1 protein or kinase-reacted hnRNP A1 protein with hTR was confirmed by competitive EMSA assay. A total of 0.1 pmol of hTR probe was bound with hnRNP A1 or kinase-reacted hnRNP A1 protein in each conditions and cold-hTR oligonucleotide was added as indicated. The signal intensity was plotted and the binding affinity was calculated in lower panel. (**C**) VRK1 deficiency resulted in reduced binding of hnRNP A1 to telomerase. The telomerase complex was immunoprecipitated with anti-TERT antibody followed by immunoblotting with anti-hnRNP A1 antibody. Knock-down of VRK1 was recovered by Flag-hVRK1 to exclude the off-target effect. Over-expression of VRK1 was confirmed by anti-VRK1 antibody and anti-Flag antibody. Telomerase activity in the hnRNP A1-depleted cell lysate was measured by direct telomerase activity assay. (**D**) After depletion of hnRNP A1, the amount of hnRNP A1 was confirmed with western blot (top panel) and GAPDH was detected for loading control (middle panel). Telomerase activity was reduced in hnRNP A1-depleted lysate (bottom panel). (**E**) HnRNP A1 or hnRNP A1 S6A mutant protein were added to the depleted extract as the indicated amount and telomerase activity was detected by autoradiography. Duplication of each samples were subjected to SDS–PAGE, followed by staining with SYPRO® Ruby protein gel staining solution.

(continued)

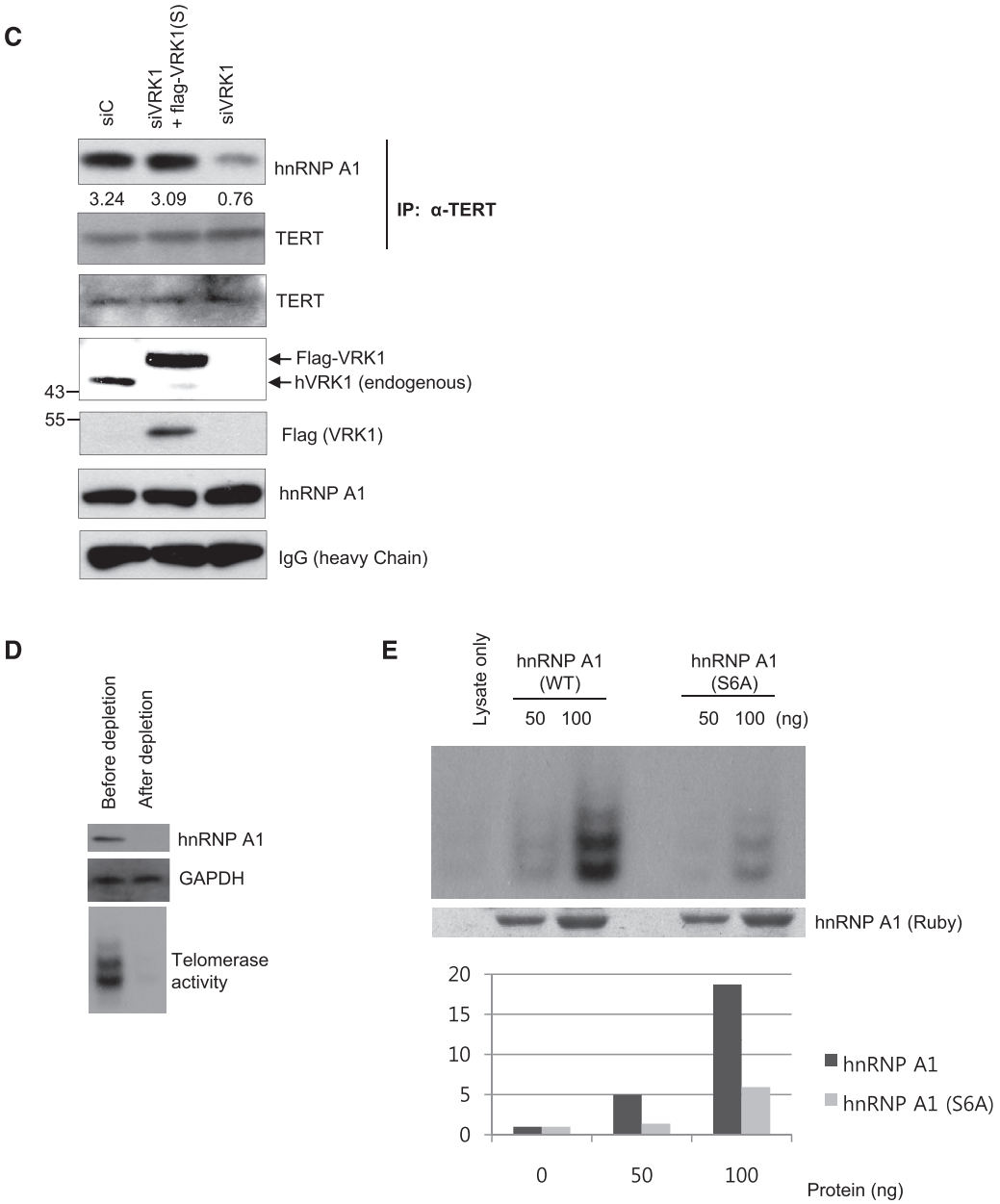

Figure 4. Continued.

7.5 h) in cells transfected with negative control siRNA (Figure 5B). Cells transfected with siVRK1 showed longer G-overhangs (>180 nt) than control cells especially in S phase (0 and 4 h). The lengthening of the G-overhang was not likely caused by the failure of cell cycle from the VRK1-knockdown, because cell cycle did not appear changed by treatment with siVRK1 (Figure 5A). As the resolution of high molecular weight (over 270 nt) was limited, we needed to confirm the result of T-OLA by other method. Therefore, we also measured 3′overhang by TRF analysis using native Southern blot (Figure 5C). In Figure 5C, 3′overhang length of VRK1-deficient cells (represented by V) was slightly increased compared to control cells (represented by C) in S and G2 phase. In each control or VRK1-deficient cells, 3′overhang length was increased by the transition from S to G2 phase. Therefore, VRK1 affects 3′overhang length in S and G2 phase.

To date, the role of hnRNP A1 in regulating the telomeric G-overhang in a cell cycle-dependent manner has not been well studied. Though the hnRNP A1 protein level appears stable during the cell cycle, we needed to assess its ability to bind telomeric ssDNA during the cell cycle. We confirmed whether the binding of hnRNP A1 to telomeric sequences changed during the cell cycle using biotinylated Telo7 oligonucleotide (Figure 5D). To prepare the synchronized cell lysates, A549 cells were released from double thymidine block at the indicated times and each sample was added to the binding reaction

with biotinylated Telo7 oligonucleotide. Figure 5D shows that hnRNP A1 binding dynamically changed during the cell cycle. In S phase (0.5 h), hnRNP A1 weakly bound to the Telo7 oligonucleotide; the binding was increased in G2 and M phase (5–9 h after release from double thymidine block).

Next, we asked whether the phosphorylation of hnRNP A1 is affected by VRK1 in a cell cycle-specific manner.

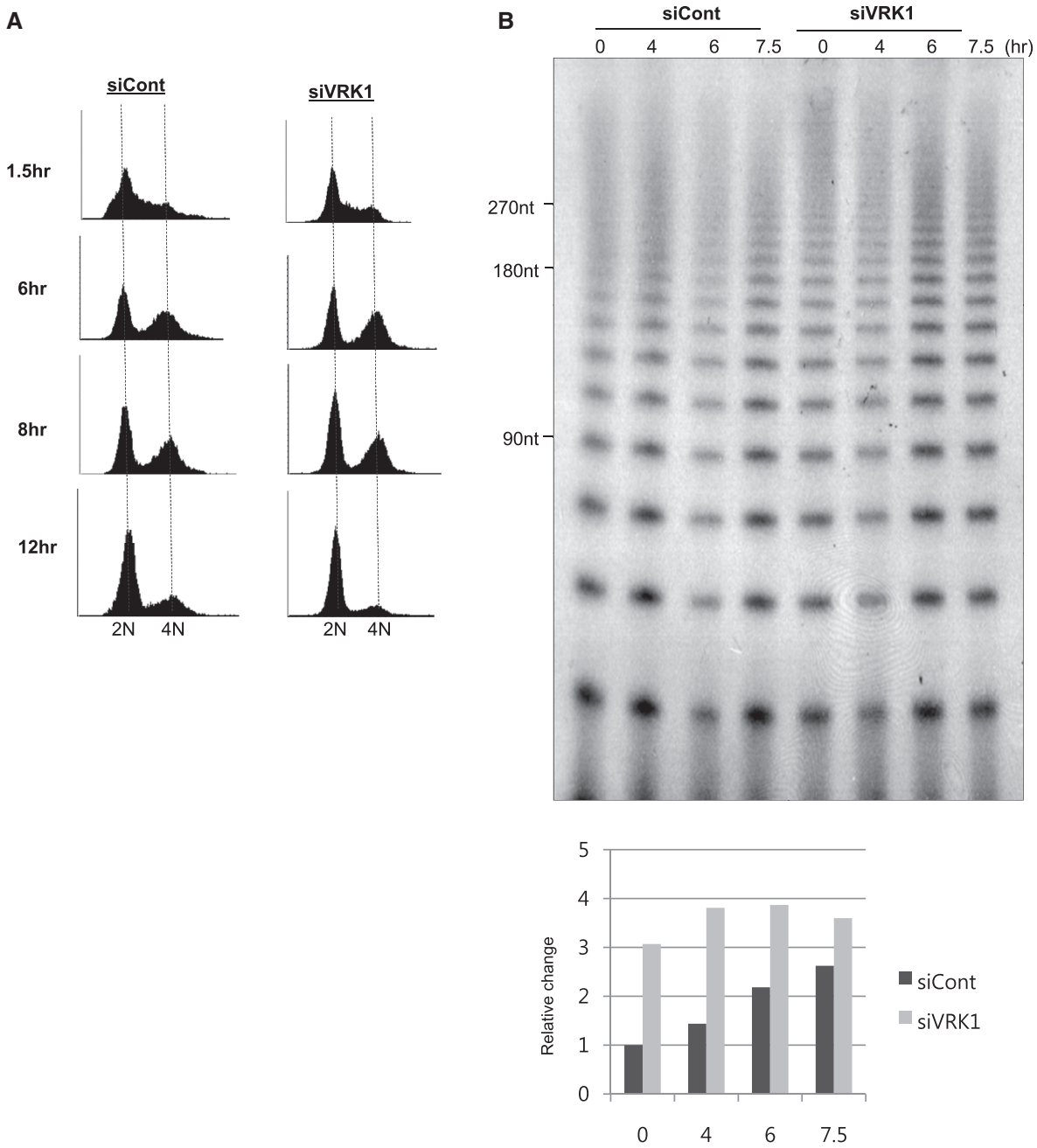

Figure 5. VRK1 deficiency results the defect on G-overhang length along the cell cycles. A549 cells transfected with negative control siRNA (siCont) or VRK1 siRNA were synchronized at the G1/S boundary using a double thymidine block and released at the indicated times. (**A**) DNA content in cells was analyzed using flow cytometry. (**B**) Length of telomeric G-overhang in siCont or siVRK1-transfected cells was analyzed with the T-OLA method described in the 'Materials and Methods' section. Each signals were normalized to time = 0 and qPCR value of GAPDH. (**C**) G-overhangs in S or G2 arrested cells, which were transfected with control siRNA or siRNA targeting VRK1, were visualized in native Southern blotting. As a control, same membrane was denaturated and reprobed with the $(CCCTAA)_3$ probe to visualize total telomeres. (**D**) A549 cells were synchronized using a double thymidine block and released at the indicated times. Proteins along the cell cycle transition were detected as an input panel (right panel). Each lysate (20 μg) was incubated with 3′-biotinylated Telo7, and bound hnRNP A1 on Telo7 was detected with western blotting. The results from individual experiments ($n = 3$) were plotted (left bottom panel). Error bars represent standard deviation. (**E**) Control (siC) or VRK1-deficient (siV) A549 cells were synchronized in G1/S or G2/M phase with hydroxyurea or nocodazole, respectively. For labeling of phosphorylated hnRNP A1, inorganic ^{32}P-phosphorus was added in a culture medium. Phosphorylation of hnRNP A1 was detected by autoradiography (^{32}P).

(continued)

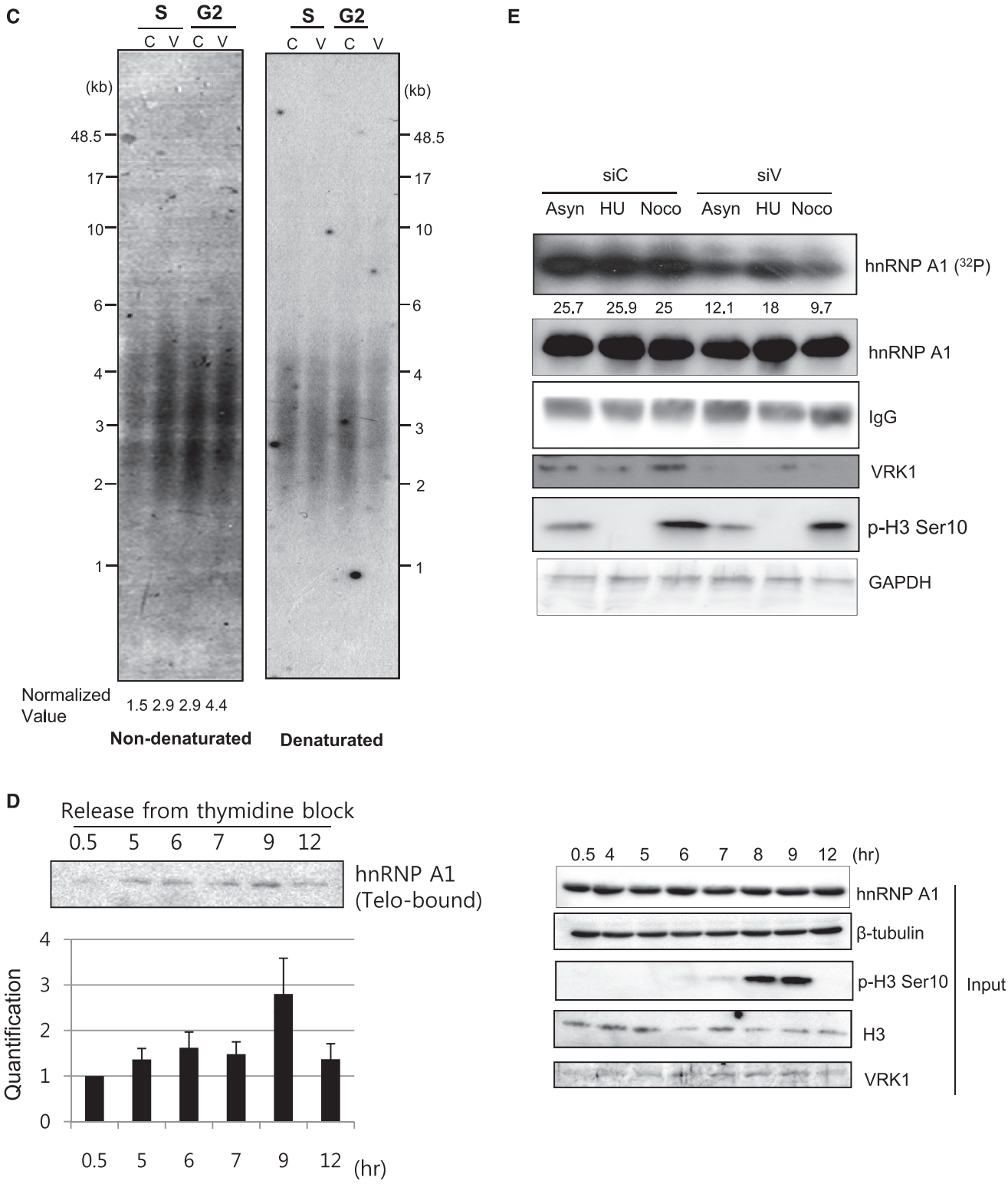

Figure 5. Continued.

Cell cycle of A549 cells was arrested at G1/S phase and G2/M phase using hydroxyurea and nocodazole, respectively. In Figure 5E, when VRK1 is depleted with siRNA, phosphorylation of hnRNP A1 is significantly decreased at G2/M phase. In G1/S phase, phosphorylation of hnRNP A1 was slightly reduced by the deficiency of VRK1. Therefore, phosphorylation of hnRNP A1 is mainly affected by VRK1 in G2/M phase, correlated with increased binding of hnRNP A1 onto telomeric ssDNA in G2/M phase.

VRK1-deficiency affects telomere integrity in mouse germ cells

Previously, we showed that VRK1 is critical for the maintenance of male germ cells (40). VRK1-deficiency causes the inhibition of germ cell proliferation, resulting in progressive germ cell loss by apoptosis (40,41). To confirm co-expression of VRK1 and hnRNP A1 in testicular cells, we performed immunohistochemistry. We monitored the distribution of VRK1 and hnRNP A1 in cancer cells and found that VRK1 and hnRNP A1 are mainly expressed in the nucleus of the human lung cancer cell line, A549, as previously reported (Figure 6A). In testis, spermatogonia expressed both VRK1 and hnRNP A1, but Sertoli cells expressed only hnRNP A1 (Figure 6B).

To assess whether VRK1 deficiency affects telomere integrity, we compared the telomere length of testicular cells in wild-type and VRK1-deficient mice by TRF analysis. The integrity of genomic DNA was confirmed by the electrophoresis (Supplementary Figure S4A and B). In Figure 6D, the mean of telomere length of VRK1-deficient cells ($n = 4$) were 18.52 kb, whereas that of wild-type cells ($n = 3$) was 20.85 kb, showing significant decrease in VRK1-deficient testicular cells (Figure 6D). In this assay (Figure 6D and Supplementary Figure S4A), we noticed that bulk of telomere signals in VRK1-deficient testes look heterogeneous. Within the same mutant strain, there was some inter-animal variation of severity of the testicular shrinkage. Therefore, it can be suggested that there is phenotypic, and probably genetic heterogeneity among mouse testicular cells derived from VRK1-deficient mice. It would be needed to find whether the severity of phenotype is related with the telomere length in further experiments.

We also investigated telomere arrangement in meiotic germ cells in VRK1-deficient mice (Figure 6C). To stain telomeres, testes sections from wild-type and VRK1-deficient mice were hybridized with fluorescein isothiocyanate-labeled peptide-nucleic acid probe. Spermatocytes (pachytene–diplotene) from wild-type mice showed that telomeres were located at peripheral areas of the nucleus (42). Compared to wild-type, telomeres of VRK1-deficient spermatocytes were dispersed in the nucleus and the intensity of telomeric signal was weak, indicating short telomere length. Furthermore, we frequently observed a chromosome bridge in mitotic germ cells from VRK1-deficient testes (WT = 1.5% and VRK1-deficient = 34.38; P-value = 0.04). In conclusion, VRK1-deficiency results in a defect in telomere length and arrangement in male germ cells.

Next, we examined whether the binding of hnRNP A1 on telomere is changed in VRK1-deficient testicular cells using telomere-ChIP assay (Figure 6E). A total of 2×10^7 cells from wild-type and VRK1-deficient testes were used for each IP conditions. In Figure 6E, binding of hnRNP A1 was decreased in VRK1-deficient cells (WT testes = 79.39% and VRK1-deficient testes = 34.38%), suggesting that phosphorylation of hnRNP A1 by VRK1 is needed for its binding to telomere *in vivo*.

Telomere instability activates DNA damage signaling, resulting in apoptosis (43–46). To assess the effect of VRK1-deficiency on DNA damage signaling, we performed immunoblotting with wild-type and VRK1-deficient testes samples. In Supplementary Figure S5A, phosphorylation of p53 at Ser 15 and Ser 20 was significantly increased in VRK1-deficient testis; as further analysis, we assessed phosphorylation of H2A.X, a marker of DNA damage (Supplementary Figure S5B). In wild-type testes, meiotic germ cells showed faint phosphorylated H2A.X signal induced by the DNA recombination process. However, the signal in VRK1-deficient testes was greatly increased compared to wild-type, demonstrating that the DNA damage signaling pathway was strongly activated in VRK1-deficient testes.

There is a possibility that the telomere abnormality in VRK1-deficient testes is caused by telomerase dysfunction. Several reports have suggested that hnRNP A1 stimulates telomerase activity, yet it has not been reported whether post-translational modification of hnRNP A1 affects telomerase action. Therefore, we analyzed whether telomerase function was affected by VRK1 deficiency. To analyze telomerase activity, the Q-TRAP assay with SYBR green method was used (34). The lysate from A549 lung cancer cells was used for determining the standard curve and linear relationship for Q-TRAP (Figure 7A). By the linear relationship from Figure 7A, the relative telomerase activity of wild-type and VRK1-deficient testes was calculated. In figure 7B, telomerase reaction from VRK1-deficient testes was significantly reduced compared to wild-type. In addition, we confirmed by immunoblotting that TERT and hnRNP A1 protein were not reduced in VRK1-deficient testes (Figure 7C).

DISCUSSION

HnRNP A1 is phosphorylated by VRK1

Several studies have shown that hnRNP A1 is telomere-binding protein *in vitro* and *in vivo* (19,23,26). In particular, it has been suggested that hnRNP A1 contributes to telomere elongation by unwinding G-quadruplexes (26,47). Although there is much evidence for a telomere regulating function of hnRNP A1, critical limitations made this role difficult to assess *in vivo*. HnRNP A1 is an abundant nuclear protein participating in a broad-range of functions that influence gene expression; thus, one could speculate that hnRNP A1 is regulated by post-translational modification. HnRNP A1 has been reported to be phosphorylated by many protein kinases including protein kinase C (PKC) (30), casein kinase II (30), protamine kinase, protein kinase A (29,30), Mnks (37) and DNA-PK (33). It has been generally understood that phosphorylation of hnRNP A1 negatively regulates its binding to target oligonucleotide sequences. For example, phosphorylation of hnRNP A1 by PKA and PKC attenuates the strand annealing activity (29,30). Mnk1 phosphorylates hnRNP A1 at Ser192 and Ser310–312 in immune cells, reducing its binding to the AU-rich element in the 3′ untranslated region of tumor necrosis

factor alpha mRNA (37). However, the role of phosphorylated hnRNP A1 in the regulation of telomere structure has not been well studied. Recently, it has been suggested that DNA-PK, stimulated by telomerase RNA, phosphorylates hnRNP A1 at Ser 95 and Ser 192 (33). In this study, phosphorylation of hnRNP A1 was diminished after treatment with DNA-PK inhibitors, suggesting that DNA-PK phosphorylates hnRNP A1 *in vivo*. Although phosphorylated hnRNP A1 is thought to have specific functions at telomeres, it is not yet known if this event contributes to telomere maintenance.

In this study, we showed that hnRNP A1 is phosphorylated by VRK1 and its phosphorylation enhances the binding affinity to telomeric sequences. We showed that VRK1 phosphorylates hnRNP A1 at sites, including Ser 6, which were identified as phosphorylated *in vivo* via global proteomic profiling of phosphopeptides (48–50). We believe that this is the first report of a phosphorylation event that enhances the binding of hnRNP A1 to telomeric single-stranded DNA. Known phosphorylation sites of hnRNP A1 inhibiting its binding to oligonucleotides are near RNA recognition motifs (Ser95 and Ser192) or in

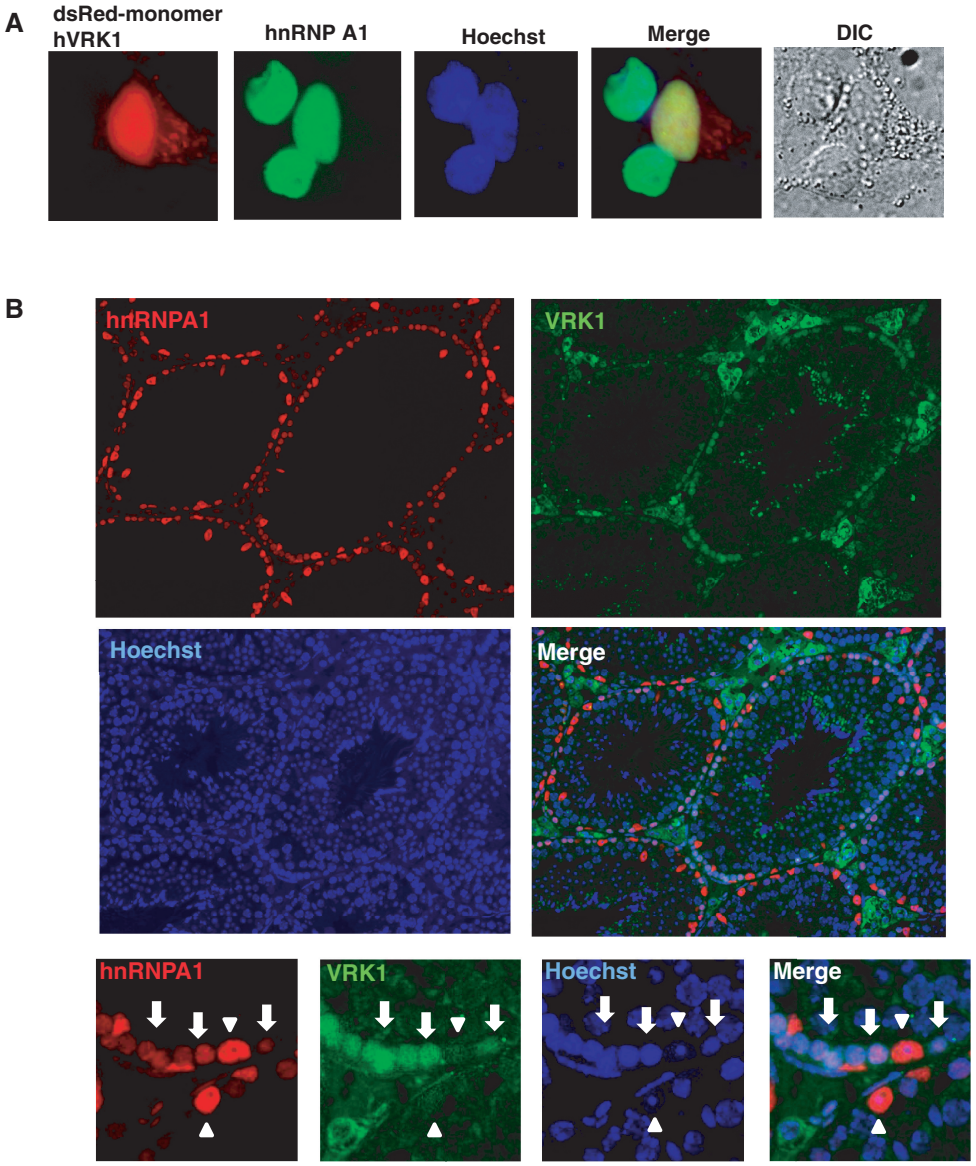

Figure 6. VRK1 affects telomere homeostasis in male mouse germ cells. (**A**) VRK1 and hnRNP A1 localize in the nucleus. dsRED-monomer-hVRK1 was transfected into A549 cells, and cells were further stained with anti-hnRNP A1 antibody. (**B**) VRK1 and hnRNP A1 were co-expressed in spermatogonia. Cross-section of adult mouse testis was immunostained with anti-mouse VRK1 and anti-hnRNP A1 antibody (arrow and arrowhead indicate spermatogonia and Sertoli cells, each). (**C**) Fluorescence in situ hybridization analysis of testis sections from wild-type and VRK1-deficient mice. (SG, spermatogonia; PL-SPC, preleptotene spermatocyte; P-SPC, parchytene spermatocyte; R-SPD; round spermatid). (**D**) Telomere length was analyzed with the genomic DNA of wild type ($n = 3$) and VRK1-deficient testes ($n = 6$) by Southern blot of TRFs. The mean of telomere length was calculated by $\sum(OD_i)/\sum(OD_i/MW_i)$. (E) Telomere-ChIP (T-ChIP) assay with WT and VRK1-deficient testicular lysates. Cells were fixed with formaldehyde followed by sonication. Sonicated samples were immunoprecipitated with non-specific serum (NS) or anti-hnRNP A1 antibodies (A1). Total sample (5%) was applied for input. T-ChIP was confirmed by two times of individual experiments and the representative result was presented. Telomeric DNA in ChIP (%) = Telomeric DNA signals of ppt/Telomeric DNA signals of input × 100%.

(continued)

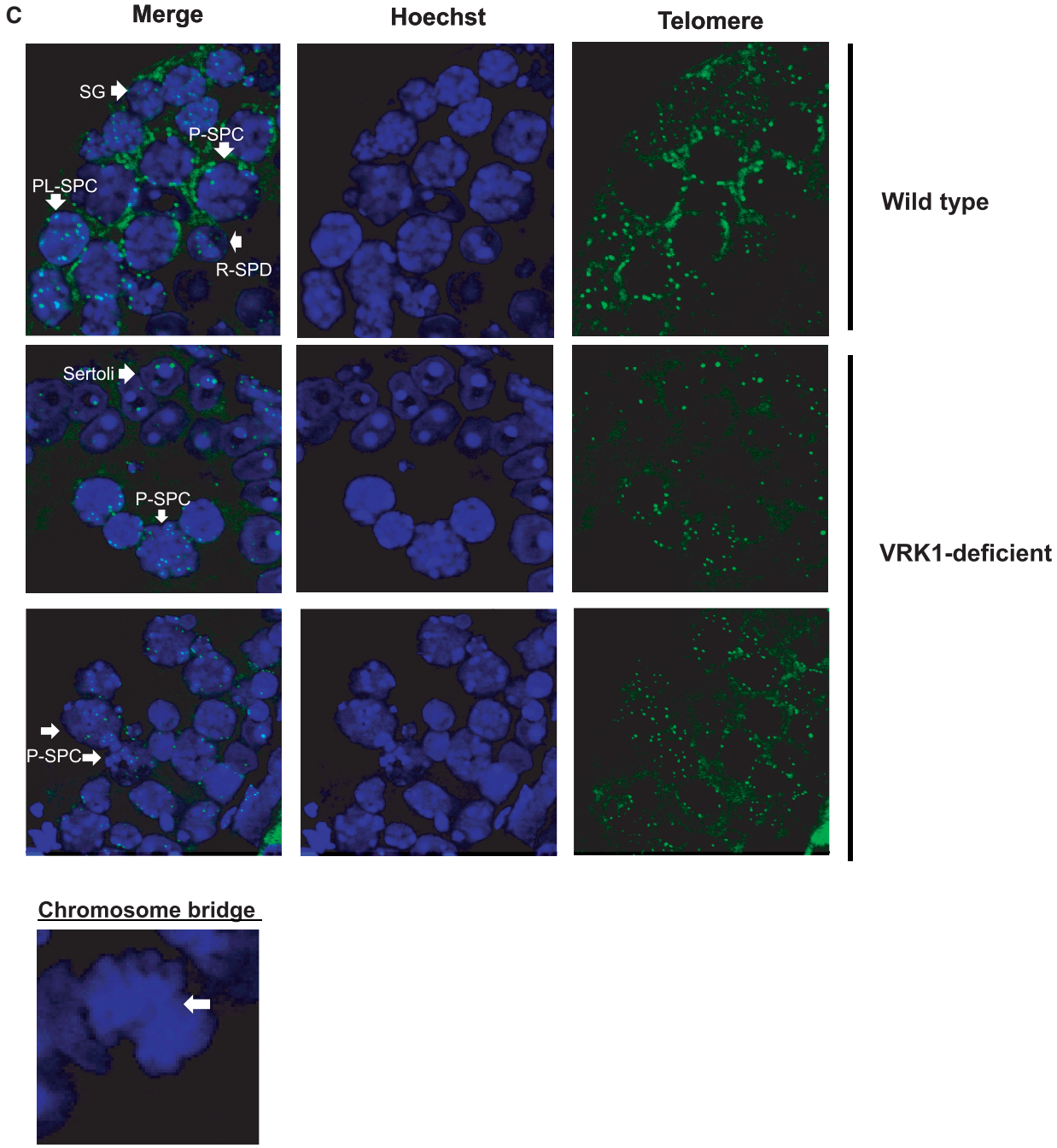

Figure 6. Continued

glycine-rich domain (Ser199, Ser310–312) which are necessary for DNA binding. As the phosphorylation of N-terminal region of hnRNP A1 has not been reported, we imagine that phosphorylation of N-terminal region affect protein structure of hnRNP A1 acquiring high affinity to polynucleotides without repelling by negative charge of DNA backbone.

Our data also show that phosphorylation of hnRNP A1 affects binding to telomerase RNA and hnRNP A1 phosphorylation at Ser6 is needed for the stimulation of the telomerase reaction. HnRNP A1/UP1 has been proposed to unwind the G-G hairpin or G-quadruplex structure contributing the processive telomere extension (26,51,52). As of yet, there is no evidence that VRK1-mediated phosphorylation of hnRNP A1 affects the unwinding of G-quadruplex, a point that needs to be clarified. On the other hand, it has been proposed that hnRNP A1 stimulates telomerase action by recruiting telomerase to telomeres (27,36). We observed that VRK1-mediated phosphorylation of hnRNP A1 also enhances its binding to telomerase RNA *in vitro* and telomerase complex *in vivo*; thus, it is possible that phosphorylated hnRNP A1 effectively recruits the telomerase complex to the telomere via enhanced

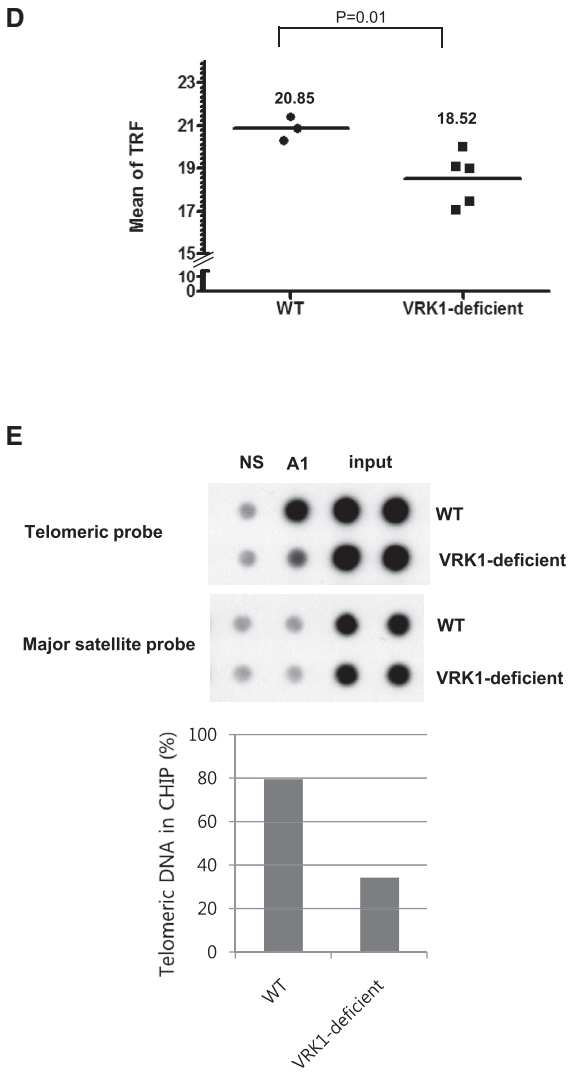

Figure 6. Continued.

binding affinity. In our data, direct telomerase assay and TRAP assay showed telomerase activity of human cancer cell line and mouse VRK1-deficient testicular cells was reduced compared to wild-type. The result from direct telomerase assay shows that hnRNP A1 activates the catalytic activity of telomerase and phosphorylation at Ser6 is critical in this process. However, whether phosphorylation of hnRNP A1 contributes telomerase processivity is not clarified in our experimental condition. For the clarification of this issue, it would be needed to analyze the effect of hnRNP A1 phosphorylation on telomerase activity with pulse chase experiment.

Cell cycle regulating protein kinase VRK1 participates in telomere length homeostasis

VRK is a new subfamily of serine–threonine kinases in the human kinome having sequence homology in its catalytic domain with the B1R kinase of Vaccinia virus (53). Among the three subfamilies of VRKs, VRK1 is well known as a cell cycle regulating kinase in mitotic progression. VRK1 is highly expressed in the G2/M phase of the cell cycle and phosphorylates histone H3 at Thr3 and Ser10, contributing to mitotic chromosome condensation (54). Barrier-to-autointegration factor (BAF) is another important substrate of VRK1 and phosphorylation of BAF results in the dissociation of chromatin from the nucleus membrane and contributes progression into the mitotic chromosome condensation (55). In addition to G2/M transition, several reports suggest that VRK1 also plays a role in G0/G1 (56) and G1/S progression (57,58). VRK1 enhances cyclin D1 gene transcription via phosphorylation of cAMP response element-binding protein (57). Consistent with VRK1 being implicated in the proliferation process, VRK1 is highly expressed in proliferating cells, such as cancer cells, embryonic cells, hematopoietic cells and male germ cell progenitors (53,59,60). Recently, a hypomorphic mouse model for VRK1 showed infertility in both sexes, suggesting that VRK1 plays a crucial role in germ cell development (40,41,61).

In this paper, we suggest that VRK1 also plays a crucial role for telomere homeostasis by phosphorylation of hnRNP A1. The expression of VRK1 oscillates dramatically during the cell cycle, showing the highest protein level in G2/M phase. We observed that deficiency of VRK1 reduces the phosphorylation of hnRNP A1 in G2/M phase rather than G1/S phase. This observation suggests that VRK1 mainly phosphorylates hnRNP A1 in G2/M phase. According to our data, binding of hnRNP A1 to telomeric ssDNA fluctuated throughout the cell cycle, even though levels of hnRNP A1 were constant. Therefore, we assumed that binding of hnRNP A1 to telomeric ssDNA was influenced by cell cycle-dependent post-translational modification. Our data show that binding of hnRNP A1 was increased during G2/M phase, corresponding with the high expression of VRK1. Together, these data suggest that the binding of hnRNP A1 to telomeric DNA is stimulated by VRK1-mediated phosphorylation in G2/M phase.

A recent report showed that hnRNP A1 displaces RPA from telomeric ssDNA in a cell cycle-dependent manner (18). Telomeric ssDNA contains bound RPA in S phase and RPA is displaced by hnRNP A1 in G2/M phase. These authors suggested that hnRNP A1 binding to telomeric ssDNA is regulated by the amount of TERRA available. In addition, we have shown that phosphorylation of hnRNP A1 itself can be an important regulating step in binding to telomeric ssDNA. VRK1-mediated phosphorylation of hnRNP A1 specifically enhances its binding to telomeric ssDNA, but has relatively little influence on TERRA. Therefore, phosphorylated hnRNP A1 may preferentially interact with telomeres, resulting in a delay in sequestration of hnRNP A1 to TERRA. Furthermore, our data showed that VRK1 deficiency resulted in an over-lengthening of the G-overhang in part; we speculate that phosphorylation of hnRNP A1 would be needed to inhibit over-lengthening of the G-overhang. Given that POT1 loss leads to an increase in G-overhang length (62), our results further suggest

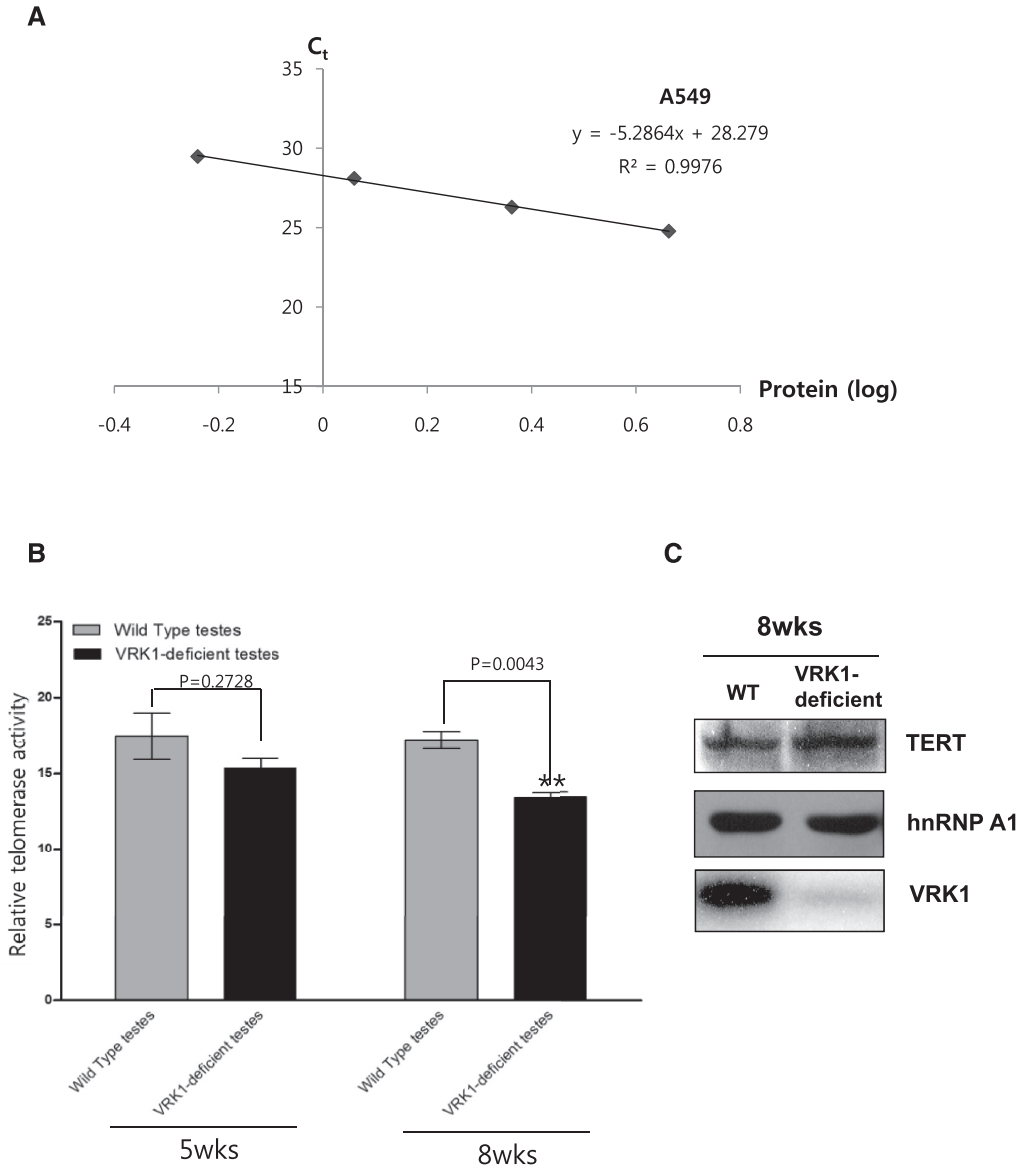

Figure 7. Telomerase activity of wild-type and VRK1-deficient testes. (**A**) Determination of the standard curve and linear relationship for Q-TRAP. The C_t values of the standard control were plotted against log[protein] to calculate the linear equation. The Y-intercept and the slope values from the equation are used to quantify the relative telomerase activity of unknown samples ($=10[(C_{t\ sample} - Y_{intercept})/slope]$). (**B**) Relative telomerase activity of 5- and 8-week-old testes from wild-type and VRK1-deficient mice were calculated using the standard curve. The samples were plotted as RTA ± SE. (**C**) Total cell lysates from 8-week-old mouse testes of wild-type and VRK1-deficient mice were analyzed by western blot.

that phosphorylation of hnRNP A1 by VRK1 might affect to the exquisite regulation of RPA-to-POT1 switching.

VRK1 is needed for the maintenance of telomere integrity in male germ cells

In a previous report, we suggested that VRK1 is needed for the maintenance of mouse male germ cells (40). Deficiency of VRK1 results in the apoptotic death of germ cells, and we have now shown that this apoptotic cell death was also caused by telomere abnormality. Germ cells lacking VRK1 showed shortening of telomeres and abnormal telomere arrangement. We observed the binding of hnRNP A1 on the telomere is reduced in VRK1-deficient testes, suggesting that VRK1-mediated phosphorylation of hnRNP A1 is important for the maintenance of telomere in germ line. Correlated with spermatogonia express VRK1 and hnRNP A1 simultaneously, VRK1-deficient mice shows the extensive loss of germ cell including spermatogonia. Sertoli cells which express hnRNP A1, but not VRK1, differentiated normally showing that VRK1 do not affect the proliferation and development of Sertoli cell. In previous study, we observed that spermatogonial stem cells express VRK1, however, whether it expresses hnRNP A1 is not known. So, it remains to resolve whether VRK1-hnRNP A1 signaling affects the telomere maintenance during the proliferation of spermatogonial stem cells.

Most mammalian somatic cells do not have sufficient telomerase activity for maintaining telomere length in every cell division, resulting the progressive shortening of telomeres (63,64). On the other hands, specific types of cells including germ line cells retain high telomerase activity in adult. Telomerase activity is crucial for the viability of germ line, as evidenced by the progressive infertility of telomerase deficient mice (65,66). As telomerase activity in VRK1-deficient testicular lysates was slightly reduced, diminished telomerase activity could be one of the causes for telomere abnormality in germ cells. Considering the progressive shortening of telomeres and loss of germ cells in telomerase knock-out mice (65,66), regulation of telomerase activity by the VRK1-hnRNP A1 pathway is thought to be crucial for germ cell maintenance. However, it cannot be excluded that telomere dysfunction was induced by telomerase-independent mechanisms, because of mild reduction of telomerase activity in VRK1-deficient testes. Although it is possible that hnRNP A1 regulates RPA-POT1 switching in mouse germ cells in consistent with human somatic cells, the difference of shelterin complex in mouse may result an organism-specific mechanism. For example, in mouse, POT1 proteins, POT1a and POT1b, are functionally distinct and partially compensate each other (67). POT1a mainly plays a role in repressing the telomere DNA damage response. On the other hand, POT1b controls telomerase-independent processing of the telomere terminus. Therefore, it remains to be solved the switching mechanism of RPA-POT1 proteins and shelterin regulation in germ cells and the relationship between VRK1 and shelterin complex.

Although the pattern of VRK1 expression correlates with cells in active proliferation in the mouse, VRK1-deficient mice do not show phenotypic changes other than in the reproductive organs. The lack of apparent changes could be due to other proteins that substitute for the function of VRK1, or the fact that 15–20% of the mutant VRK1 strains are leaky, providing enough protein to perform the function (40,41). Our data showed that VRK1 deficiency in the A549 lung cancer cell line did not significantly disturb the cell cycle for up to 48 h. However, previous experiments with the human fibroblast cell line, WS1, showed that loss of VRK1 resulted in a blockage of cell cycle progression in G1/S (56). This discrepancy might be caused by the efficiency of knock-down of VRK1 using siRNA, and/or the difference in cell lines, which may not both have VRK1 as a main cell cycle regulating kinase. Even though VRK1 is not completely depleted in the A549 cell line and in VRK1-deficient testes, the reduction appears sufficient to induce a severe defect on telomere integrity.

In summary, we suggest that VRK1 participates in the maintenance of telomeres by phosphorylating hnRNP A1, which enhances binding to telomere ssDNA and telomerase RNA. Moreover, VRK1 is needed for the proper regulation of G-overhang length and telomere integrity of mouse male germ cells. These results strongly suggest that VRK1 can be an important mediator between cell cycle and regulation of telomere integrity.

SUPPLEMENTARY DATA

Supplementary Data are available at NAR Online: Supplementary Figures 1–5.

FUNDING

The Core Research Program/Anti-aging and Well-being Research Center, the Brain Korea 21 program, and World Class University program [R31-10105] of the Ministry of Education, Science and Technology. Funding for open access charge: The National Research Foundation of Korea (NRF); [20100002146, 20100019706, 20100030089 and 20110031517].

Conflict of interest statement. None declared.

REFERENCES

1. McEachern,M.J., Krauskopf,A. and Blackburn,E.H. (2000) Telomeres and their control. *Annu. Rev. Genet.*, **34**, 331–358.
2. Makarov,V.L., Hirose,Y. and Langmore,J.P. (1997) Long G tails at both ends of human chromosomes suggest a C strand degradation mechanism for telomere shortening. *Cell*, **88**, 657–666.
3. Wright,W.E., Tesmer,V.M., Huffman,K.E., Levene,S.D. and Shay,J.W. (1997) Normal human chromosomes have long G-rich telomeric overhangs at one end. *Genes Dev.*, **11**, 2801–2809.
4. McElligott,R. and Wellinger,R.J. (1997) The terminal DNA structure of mammalian chromosomes. *EMBO J.*, **16**, 3705–3714.
5. Palm,W. and de Lange,T. (2008) How shelterin protects mammalian telomeres. *Annu. Rev. Genet.*, **42**, 301–334.
6. Nikitina,T. and Woodcock,C.L. (2004) Closed chromatin loops at the ends of chromosomes. *J. Cell Biol.*, **166**, 161–165.
7. Griffith,J.D., Comeau,L., Rosenfield,S., Stansel,R.M., Bianchi,A., Moss,H. and de Lange,T. (1999) Mammalian telomeres end in a large duplex loop. *Cell*, **97**, 503–514.
8. de Lange,T. (2005) Shelterin: the protein complex that shapes and safeguards human telomeres. *Genes Dev.*, **19**, 2100–2110.
9. Verdun,R.E. and Karlseder,J. (2006) The DNA damage machinery and homologous recombination pathway act consecutively to protect human telomeres. *Cell*, **127**, 709–720.
10. Larrivee,M., LeBel,C. and Wellinger,R.J. (2004) The generation of proper constitutive G-tails on yeast telomeres is dependent on the MRX complex. *Genes Dev.*, **18**, 1391–1396.
11. Zhao,Y., Sfeir,A.J., Zou,Y., Buseman,C.M., Chow,T.T., Shay,J.W. and Wright,W.E. (2009) Telomere extension occurs at most chromosome ends and is uncoupled from fill-in in human cancer cells. *Cell*, **138**, 463–475.
12. Dai,X., Huang,C., Bhusari,A., Sampathi,S., Schubert,K. and Chai,W. (2010) Molecular steps of G-overhang generation at human telomeres and its function in chromosome end protection. *EMBO J.*, **29**, 2788–2801.
13. Bonetti,D., Martina,M., Clerici,M., Lucchini,G. and Longhese,M.P. (2009) Multiple pathways regulate 3′ overhang generation at *S. cerevisiae telomeres*. *Mol. Cell*, **35**, 70–81.
14. Frank,C.J., Hyde,M. and Greider,C.W. (2006) Regulation of telomere elongation by the cyclin-dependent kinase CDK1. *Mol. Cell*, **24**, 423–432.
15. Vodenicharov,M.D. and Wellinger,R.J. (2006) DNA degradation at unprotected telomeres in yeast is regulated by the CDK1 (Cdc28/Clb) cell-cycle kinase. *Mol. Cell*, **24**, 127–137.
16. Zou,L. and Elledge,S.J. (2003) Sensing DNA damage through ATRIP recognition of RPA-ssDNA complexes. *Science*, **300**, 1542–1548.
17. Churikov,D. and Price,C.M. (2008) Pot1 and cell cycle progression cooperate in telomere length regulation. *Nat. Struct. Mol. Biol.*, **15**, 79–84.
18. Flynn,R.L., Centore,R.C., O'Sullivan,R.J., Rai,R., Tse,A., Songyang,Z., Chang,S., Karlseder,J. and Zou,L. (2011) TERRA

and hnRNPA1 orchestrate an RPA-to-POT1 switch on telomeric single-stranded DNA. *Nature*, **471**, 532–536.
19. Ishikawa,F., Matunis,M.J., Dreyfuss,G. and Cech,T.R. (1993) Nuclear proteins that bind the pre-mRNA 3′ splice site sequence r(UUAG/G) and the human telomeric DNA sequence d(TTAGG G)n. *Mol. Cell Biol.*, **13**, 4301–4310.
20. McKay,S.J. and Cooke,H. (1992) hnRNP A2/B1 binds specifically to single stranded vertebrate telomeric repeat TTAGGGn. *Nucleic Acids Res.*, **20**, 6461–6464.
21. Abdul-Manan,N. and Williams,K.R. (1996) hnRNP A1 binds promiscuously to oligoribonucleotides: utilization of random and homo-oligonucleotides to discriminate sequence from base-specific binding. *Nucleic Acids Res.*, **24**, 4063–4070.
22. Sarig,G., Weisman-Shomer,P., Erlitzki,R. and Fry,M. (1997) Purification and characterization of qTBP42, a new single-stranded and quadruplex telomeric DNA-binding protein from rat hepatocytes. *J. Biol. Chem.*, **272**, 4474–4482.
23. LaBranche,H., Dupuis,S., Ben-David,Y., Bani,M.R., Wellinger,R.J. and Chabot,B. (1998) Telomere elongation by hnRNP A1 and a derivative that interacts with telomeric repeats and telomerase. *Nat. Genet.*, **19**, 199–202.
24. Dallaire,F., Dupuis,S., Fiset,S. and Chabot,B. (2000) Heterogeneous nuclear ribonucleoprotein A1 and UP1 protect mammalian telomeric repeats and modulate telomere replication in vitro. *J. Biol. Chem.*, **275**, 14509–14516.
25. Ding,J., Hayashi,M.K., Zhang,Y., Manche,L., Krainer,A.R. and Xu,R.M. (1999) Crystal structure of the two-RRM domain of hnRNP A1 (UP1) complexed with single-stranded telomeric DNA. *Genes Dev.*, **13**, 1102–1115.
26. Zhang,Q.S., Manche,L., Xu,R.M. and Krainer,A.R. (2006) hnRNP A1 associates with telomere ends and stimulates telomerase activity. *RNA*, **12**, 1116–1128.
27. Nagata,T., Takada,Y., Ono,A., Nagata,K., Konishi,Y., Nukina,T., Ono,M., Matsugami,A., Furukawa,A., Fujimoto,N. *et al.* (2008) Elucidation of the mode of interaction in the UP1-telomerase RNA-telomeric DNA ternary complex which serves to recruit telomerase to telomeric DNA and to enhance the telomerase activity. *Nucleic Acids Res.*, **36**, 6816–6824.
28. Li,T., Evdokimov,E., Shen,R.F., Chao,C.C., Tekle,E., Wang,T., Stadtman,E.R., Yang,D.C. and Chock,P.B. (2004) Sumoylation of heterogeneous nuclear ribonucleoproteins, zinc finger proteins, and nuclear pore complex proteins: a proteomic analysis. *Proc. Natl Acad. Sci. USA*, **101**, 8551–8556.
29. Cobianchi,F., Calvio,C., Stoppini,M., Buvoli,M. and Riva,S. (1993) Phosphorylation of human hnRNP protein A1 abrogates in vitro strand annealing activity. *Nucleic Acids Res.*, **21**, 949–955.
30. Idriss,H., Kumar,A., Casas-Finet,J.R., Guo,H., Damuni,Z. and Wilson,S.H. (1994) Regulation of in vitro nucleic acid strand annealing activity of heterogeneous nuclear ribonucleoprotein protein A1 by reversible phosphorylation. *Biochemistry*, **33**, 11382–11390.
31. Municio,M.M., Lozano,J., Sanchez,P., Moscat,J. and Diaz-Meco,M.T. (1995) Identification of heterogeneous ribonucleoprotein A1 as a novel substrate for protein kinase C zeta. *J. Biol. Chem.*, **270**, 15884–15891.
32. van der Houven van Oordt,W., Diaz-Meco,M.T., Lozano,J., Krainer,A.R., Moscat,J. and Caceres,J.F. (2000) The MKK(3/6)-p38-signaling cascade alters the subcellular distribution of hnRNP A1 and modulates alternative splicing regulation. *J. Cell Biol.*, **149**, 307–316.
33. Ting,N.S., Pohorelic,B., Yu,Y., Lees-Miller,S.P. and Beattie,T.L. (2009) The human telomerase RNA component, hTR, activates the DNA-dependent protein kinase to phosphorylate heterogeneous nuclear ribonucleoprotein A1. *Nucleic Acids Res.*, **37**, 6105–6115.
34. Herbert,B.S., Hochreiter,A.E., Wright,W.E. and Shay,J.W. (2006) Nonradioactive detection of telomerase activity using the telomeric repeat amplification protocol. *Nat. Protoc.*, **1**, 1583–1590.
35. Cimino-Reale,G., Pascale,E., Battiloro,E., Starace,G., Verna,R. and D'Ambrosio,E. (2001) The length of telomeric G-rich strand 3′-overhang measured by oligonucleotide ligation assay. *Nucleic Acids Res.*, **29**, E35.
36. Fiset,S. and Chabot,B. (2001) hnRNP A1 may interact simultaneously with telomeric DNA and the human telomerase RNA in vitro. *Nucleic Acids Res.*, **29**, 2268–2275.
37. Buxade,M., Parra,J.L., Rousseau,S., Shpiro,N., Marquez,R., Morrice,N., Bain,J., Espel,E. and Proud,C.G. (2005) The Mnks are novel components in the control of TNF alpha biosynthesis and phosphorylate and regulate hnRNP A1. *Immunity*, **23**, 177–189.
38. Xue,Y., Ren,J., Gao,X., Jin,C., Wen,L. and Yao,X. (2008) GPS 2.0, a tool to predict kinase-specific phosphorylation sites in hierarchy. *Mol. Cell Proteomics*, **7**, 1598–1608.
39. Manning,G., Whyte,D.B., Martinez,R., Hunter,T. and Sudarsanam,S. (2002) The protein kinase complement of the human genome. *Science*, **298**, 1912–1934.
40. Choi,Y.H., Park,C.H., Kim,W., Ling,H., Kang,A., Chang,M.W., Im,S.K., Jeong,H.W., Kong,Y.Y. and Kim,K.T. (2010) Vaccinia-related kinase 1 is required for the maintenance of undifferentiated spermatogonia in mouse male germ cells. *PLoS One*, **5**, e15254.
41. Wiebe,M.S., Nichols,R.J., Molitor,T.P., Lindgren,J.K. and Traktman,P. (2010) Mice deficient in the serine/threonine protein kinase VRK1 are infertile due to a progressive loss of spermatogonia. *Biol. Reprod.*, **82**, 182–193.
42. Tanemura,K., Ogura,A., Cheong,C., Gotoh,H., Matsumoto,K., Sato,E., Hayashi,Y., Lee,H.W. and Kondo,T. (2005) Dynamic rearrangement of telomeres during spermatogenesis in mice. *Dev. Biol.*, **281**, 196–207.
43. Celli,G.B. and de Lange,T. (2005) DNA processing is not required for ATM-mediated telomere damage response after TRF2 deletion. *Nat. Cell Biol.*, **7**, 712–718.
44. d'Adda di Fagagna,F., Reaper,P.M., Clay-Farrace,L., Fiegler,H., Carr,P., Von Zglinicki,T., Saretzki,G., Carter,N.P. and Jackson,S.P. (2003) A DNA damage checkpoint response in telomere-initiated senescence. *Nature*, **426**, 194–198.
45. Karlseder,J., Broccoli,D., Dai,Y., Hardy,S. and de Lange,T. (1999) p53- and ATM-dependent apoptosis induced by telomeres lacking TRF2. *Science*, **283**, 1321–1325.
46. Takai,H., Smogorzewska,A. and de Lange,T. (2003) DNA damage foci at dysfunctional telomeres. *Curr. Biol.*, **13**, 1549–1556.
47. Kruger,A.C., Raarup,M.K., Nielsen,M.M., Kristensen,M., Besenbacher,F., Kjems,J. and Birkedal,V. (2010) Interaction of hnRNP A1 with telomere DNA G-quadruplex structures studied at the single molecule level. *Eur. Biophys. J.*, **39**, 1343–1350.
48. Shu,H., Chen,S., Bi,Q., Mumby,M. and Brekken,D.L. (2004) Identification of phosphoproteins and their phosphorylation sites in the WEHI-231 B lymphoma cell line. *Mol. Cell Proteomics*, **3**, 279–286.
49. Dephoure,N., Zhou,C., Villen,J., Beausoleil,S.A., Bakalarski,C.E., Elledge,S.J. and Gygi,S.P. (2008) A quantitative atlas of mitotic phosphorylation. *Proc. Natl Acad. Sci. USA*, **105**, 10762–10767.
50. Molina,H., Horn,D.M., Tang,N., Mathivanan,S. and Pandey,A. (2007) Global proteomic profiling of phosphopeptides using electron transfer dissociation tandem mass spectrometry. *Proc. Natl Acad. Sci. USA*, **104**, 2199–2204.
51. Fukuda,H., Katahira,M., Tsuchiya,N., Enokizono,Y., Sugimura,T., Nagao,M. and Nakagama,H. (2002) Unfolding of quadruplex structure in the G-rich strand of the minisatellite repeat by the binding protein UP1. *Proc. Natl Acad. Sci. USA*, **99**, 12685–12690.
52. Riva,S., Morandi,C., Tsoulfas,P., Pandolfo,M., Biamonti,G., Merrill,B., Williams,K.R., Multhaup,G., Beyreuther,K., Werr,H. *et al.* (1986) Mammalian single-stranded DNA binding protein UP I is derived from the hnRNP core protein A1. *EMBO J.*, **5**, 2267–2273.
53. Nezu,J., Oku,A., Jones,M.H. and Shimane,M. (1997) Identification of two novel human putative serine/threonine kinases, VRK1 and VRK2, with structural similarity to vaccinia virus B1R kinase. *Genomics*, **45**, 327–331.
54. Kang,T.H., Park,D.Y., Choi,Y.H., Kim,K.J., Yoon,H.S. and Kim,K.T. (2007) Mitotic histone H3 phosphorylation by vaccinia-related kinase 1 in mammalian cells. *Mol. Cell Biol.*, **27**, 8533–8546.

55. Nichols,R.J., Wiebe,M.S. and Traktman,P. (2006) The vaccinia-related kinases phosphorylate the N′ terminus of BAF, regulating its interaction with DNA and its retention in the nucleus. *Mol. Biol. Cell*, **17**, 2451–2464.
56. Valbuena,A., Lopez-Sanchez,I. and Lazo,P.A. (2008) Human VRK1 is an early response gene and its loss causes a block in cell cycle progression. *PLoS One*, **3**, e1642.
57. Kang,T.H., Park,D.Y., Kim,W. and Kim,K.T. (2008) VRK1 phosphorylates CREB and mediates CCND1 expression. *J. Cell. Sci.*, **121**, 3035–3041.
58. Vega,F.M., Sevilla,A. and Lazo,P.A. (2004) p53 Stabilization and accumulation induced by human vaccinia-related kinase 1. *Mol. Cell Biol.*, **24**, 10366–10380.
59. Vega,F.M., Gonzalo,P., Gaspar,M.L. and Lazo,P.A. (2003) Expression of the VRK (vaccinia-related kinase) gene family of p53 regulators in murine hematopoietic development. *FEBS Lett.*, **544**, 176–180.
60. Santos,C.R., Rodriguez-Pinilla,M., Vega,F.M., Rodriguez-Peralto,J.L., Blanco,S., Sevilla,A., Valbuena,A., Hernandez,T., van Wijnen,A.J., Li,F. *et al.* (2006) VRK1 signaling pathway in the context of the proliferation phenotype in head and neck squamous cell carcinoma. *Mol. Cancer Res.*, **4**, 177–185.
61. Schober,C.S., Aydiner,F., Booth,C.J., Seli,E. and Reinke,V. (2011) The kinase VRK1 is required for normal meiotic progression in mammalian oogenesis. *Mech. Dev.*, **128**, 178–190.
62. Churikov,D., Wei,C. and Price,C.M. (2006) Vertebrate POT1 restricts G-overhang length and prevents activation of a telomeric DNA damage checkpoint but is dispensable for overhang protection. *Mol. Cell Biol.*, **26**, 6971–6982.
63. Flores,I., Cayuela,M.L. and Blasco,M.A. (2005) Effects of telomerase and telomere length on epidermal stem cell behavior. *Science*, **309**, 1253–1256.
64. Harley,C.B., Futcher,A.B. and Greider,C.W. (1990) Telomeres shorten during ageing of human fibroblasts. *Nature*, **345**, 458–460.
65. Lee,H.W., Blasco,M.A., Gottlieb,G.J., Horner,J.W. II, Greider,C.W. and DePinho,R.A. (1998) Essential role of mouse telomerase in highly proliferative organs. *Nature*, **392**, 569–574.
66. Herrera,E., Samper,E., Martin-Caballero,J., Flores,J.M., Lee,H.W. and Blasco,M.A. (1999) Disease states associated with telomerase deficiency appear earlier in mice with short telomeres. *EMBO J.*, **18**, 2950–2960.
67. Hockemeyer,D., Daniels,J.P., Takai,H. and de Lange,T. (2006) Recent expansion of the telomeric complex in rodents: two distinct POT1 proteins protect mouse telomeres. *Cell*, **126**, 63–77.